

**Prescribed Fire Effects on Soil Properties and Nutrient Dynamics in a Longleaf Pine
Forested Wetland Watershed**

by

Lidia Del Carmen Molina Serpas

A thesis submitted to the Graduate Faculty of Auburn University
in partial fulfillment of the
requirements for a Master of Science Degree in Geography
Auburn University

Auburn, Alabama
December 10, 2022

Keywords: Prescribed fire, Hydrological Properties, Longleaf Pine Forests, Nutrient dynamics,
Soil Properties, Geographically Isolated Wetlands

Approved by

Dr. Stephanie Shepherd, Chair, Department of Geoscience
Dr. Frances O'Donnell, Department of Civil Engineering
Dr. Matthew Waters, Department of Crop Soil and Environmental Science

ABSTRACT

In a geographically isolated wetland (GIW) area, located in Georgia, longleaf pine forests have been experiencing frequent rotational prescribed burning for more than 10 years. In general, because wetlands provide ecosystem services, such as sediment retention and nutrient storage, it is important to understand how fire can alter biogeochemical processes. Previous research has shown that prescribed fires can release nutrients, alter soil properties, and modify soil moisture dynamics. Prescribed fire effects to Longleaf pine forests have been documented in the Southeast, but few have investigated effects to forested GIWs. These studies generally focus on prescribed fire impacts to water quality. In comparison, this research studies the effects of prescribed fire on hydrological properties, soil properties, nutrient movement, as well as carbon and nitrogen isotopic ratios to further understand immediate (short-term) changes in surface and subsurface horizons as well as chronic (long-term) impacts along a low-relief hillslope where there is a transition from forest to wetland. The main objectives of this research were to: (1) document soil moisture alterations immediately after prescribe fire, in the surface horizon, (2) determine whether or not prescribed fire can increase vertical nutrient movement with depth in a soil profile over short time scales, and (3) identify the immediate and chronic effects prescribed fire will have on nutrient concentrations and carbon and nitrogen isotopic ratios in surface and subsurface soil horizons. Two forested GIW watersheds at the Jones Center at Ichauway, GA were selected for study. Both are managed with prescribed burns bi-annually, one burned during the study (immediate site) and one burned the year prior (chronic site). Sampling was conducted before the prescribed fire, after the prescribed fire, and after a large rain event. Two-way ANOVA analysis and unpaired t-tests show no significant short-term changes to hydrological properties, but shortly after the fire, hydrophobicity increased promptly after the fire in all

sampling points but only remained high on the hillslope after the rain event contrary to the expected decrease in hydrophobicity with increasing soil moisture. There were no prominent effects to soil texture and bulk density immediately after the prescribed fire or after the rain event. There were observable temporal changes to nutrient concentrations in surface and subsurface horizons and we found a positive correlation existing post-fire. The expressed significant differences in the horizons and the higher nutrient levels found in the chronic site is potentially caused by the addition of ash into the system overtime. In our immediate site, there were nutrient (total C, P, Mg, K, Ca, and Mn) increases found along the wetland edge. Also after the large rain event, total Al and Fe concentrations increased in subsurface horizons at the immediate site suggesting a fire signature. There were no significant temporal changes to carbon and nitrogen isotopic signatures despite finding some enrichment. Overall, a prescribed fire may cause immediate effects to hydrological properties, but it can also lead to chronic impacts due to the observed alterations to soil properties and nutrient dynamics. This work shows that short-term and long-term effects are difficult to resolve and specific impacts to soil nutrient cycling requires more study.

ACKNOWLEDGEMENTS

Foremost, I would like to thank the Jones Center at Ichauway for hosting my stay and allowing me to conduct my research at their station. I would like to thank Dr. Shepherd, Dr. Waters, and Dr. O'Donnell for guiding me and helping me develop my thesis. I would like to thank my family, Lilian, Carmen, Richard, Juan, and friends for their support and for inspiring me. I would also like to thank those who helped me collect data in the field (specifically Dr. Shepherd, Coleman, Dr. Golladay, Dr. O'Donnell, and Sophia). I would also like to thank Dr. Principato, Dr. Urcuyo, Dr. Hiraizumi, Dr. Trillo, and Dr. Caldwell.

LIST OF TABLES

CHAPTER 3.....27

Table 1. Unsaturated hydraulic conductivity and water repellency recorded for study sites.....40

Table 2. Nutrient concentrations in study sites for sampling time 1 (T1) and time 2 (T2).....42

APPENDIX A: SOIL PROPERTIES.....61

A.1. Soil Descriptions.....61

Table A1. Soil description from upland region before the prescribed fire retrieved from immediate site.....61

Table A2. Description of soil samples collected from transition zone 1 before the scheduled prescribed fire in immediate site.....61

Table A3. Soil description of soil core collected pre-fire at the immediate site from transition zone 2.....62

Table A4. Description of samples collected from wetland edge before the prescribed fire in immediate site.....62

Table A5. Soil description from upland area after the prescribed fire.....62

Table A6. Description of soil samples collected from transition zone 1 after the scheduled prescribed fire in immediate site.....63

Table A7. Soil description of soil core collected from transition zone 2 after the prescribed fire.....63

Table A8. Description of samples collected from wetland edge after the scheduled prescribed fire.....63

Table A9. Soil description of samples from chronic site in upland region collected before the rain event.....64

Table A10. Description of samples retrieved before the rain event from chronic site in transition zone 1.....64

Table A11. Soil description of samples retrieved before the rain event from chronic site in transition zone 2.....64

Table A12. Description of soil samples collected before the rain event from chronic site retrieved from wetland edge.....	65
Table A13. Soil description of samples from chronic site in upland area after the rain event	65
Table A14. Description of samples retrieved after the rain event from chronic site in transition zone 1.....	65
Table A15. Soil description of samples retrieved after the rain event from chronic site in transition zone 2.....	66
Table A16. Description of soil samples collected from chronic site retrieved from wetland edge after the rain event.....	66
<i>A.2. Bulk Density.....</i>	67
Table A17. Bulk density calculations.....	67
Table A18. Two-way ANOVA analysis for soil bulk density pre-fire and post-fire.....	67
Table A19 Unpaired t-test results for soil bulk density pre-fire and post-fire.....	67
<i>A.3. Grain Size Analysis.....</i>	68
Table A20. Grain size analysis data in study sites for sampling time 1.....	72
Table A21. Grain size analysis data in study sites for sampling time 2	73
Table A22. Two-way ANOVA analysis comparison for grain size in soil A horizon within samples (sampling times) and between sites (columns).....	74
Table A23. Unpaired t-test results for grain size distribution in the soil A horizon.....	74
Table A24. Two-way ANOVA analysis for grain size in soil B horizon within samples (sampling times) and between sites (columns).....	75
Table A25. Unpaired t-test results for grain size analysis in soil B horizon.....	75
APPENDIX B: HYDROLOGICAL PROPERTIES.....	76
<i>B.1. Water Infiltration Raw Data.....</i>	77
Table B1. Water infiltration data for upland area in immediate site.....	77
Table B2. Water infiltration data for transition zone 1 in immediate site.....	78

Table B3. Water infiltration data for transition zone 2 in immediate site.....	79
Table B4. Water infiltration data for wetland edge in immediate site.....	79
<i>B.2. Ethanol Infiltration Raw Data.....</i>	80
Table B5. Ethanol infiltration for upland area in immediate site.....	80
Table B6. Ethanol infiltration data for transition zone 1 in immediate site.....	81
Table B7. Ethanol infiltration data for transition zone 2 in immediate site.....	81
Table B8. Ethanol infiltration data for wetland edge in immediate site.....	82
<i>B.3. Statistical Analysis.....</i>	83
Table B9 Unpaired t-test results for unsaturated hydraulic conductivity comparisons in upland and transition zone 1 in immediate site.....	83
Table B10. Unpaired t-test results for water repellency in immediate site.....	84
APPENDIX C: NUTRIENTS.....	85
<i>C.1. Statistical Analysis</i>	85
Table C1. Unpaired t-test results for nutrients in soil A horizon.....	85
Table C2. Unpaired t-test results for nutrients in soil B horizon.....	87
Table C3. Two-way ANOVA analysis for nutrient pools in soil A horizon within samples (sampling times) and between sites (columns).....	89
Table C4. Two-way ANOVA analysis for nutrient pools in soil B horizon within samples (sampling times) and between sites (columns).....	90
Table C5. Eigenvectors values determined from principal component analysis.....	91
APPENDIX D: CARBON AND NITROGEN ISOTOPIC RATIOS	92
<i>D.1. Carbon and Nitrogen Isotopic ratios Raw Data.....</i>	92
Table D1. Carbon and nitrogen isotopic ratios in study sites.....	92

D.2. Statistical Analysis.....93

Table D2. Two-way ANOVA analysis for carbon and nitrogen isotopic ratios in soil A horizon within samples (sampling times) and between sites (columns).....93

Table D3. Two-way ANOVA analysis for carbon and nitrogen isotopic ratios in soil B horizon within samples (sampling times) and between sites (columns).....93

Table D4. Unpaired t-test results for carbon and nitrogen isotopic ratios in soil A horizon.....94

Table D5. Unpaired t-test results for carbon and nitrogen isotopic ratios in soil B horizon.....94

LIST OF FIGURES

CHAPTER 1.....	1
Figure 1. Prescribed burned areas and wildfire areas within the United States as portrayed in Mitchell et al. 2014.....	2
Figure 2. Study site at the Jones Center at Ichauway in Georgia, USA.....	4
CHAPTER 2.....	10
Figure 1. Minidisk infiltrometer apparatus.....	13
CHAPTER 3.....	27
Figure 1. Map illustrating our study area at the Jones Center at Ichauway in Georgia, USA.....	33
Figure 2. Field setup for immediate site and chronic site with established transect and soil sampling points.....	34
Figure 3. Rainfall and wetland water levels present in the immediate site.....	35
Figure 4. Principal component analysis biplot portraying nutrient pools across immediate site under pre-fire and post-fire conditions in soil A and B horizons.....	43
Figure 5. Carbon and nitrogen isotopic ratio for A horizon and B horizons in immediate and chronic site under sampling time 1 and 2.....	45
APPENDIX A: SOIL PROPERTIES.....	61
<i>A.3. Grain Size Analysis.....</i>	68
Figure A1. Grain size comparison between cores before the rain event from immediate and chronic sites.....	68
Figure A2. Grain size distribution comparison between cores taken after the rain event from immediate and chronic sites.....	70
APPENDIX B: HYDROLOGICAL PROPERTIES.....	76
Figure B1. Water and ethanol infiltration data recorded from immediate site.....	76

ABBREVIATIONS

C	Carbon
P	Phosphorus
K	Potassium
Mn	Manganese
Fe	Iron
Ca	Calcium
Mg	Magnesium
Al	Aluminum
$\delta^{13}\text{C}$	Delta 13 C(carbon)
$\delta^{15}\text{N}$	Delta 15 N(nitrogen)
GIWs	Geographically Isolated Wetlands
$\text{PO}_4\text{-P}$	Phosphate
$\text{NH}_4\text{-N}$	Ammonium

TABLE OF CONTENTS

ABSTRACT.....	II
ACKNOWLEDGEMENTS	IV
LIST OF TABLES.....	V
LIST OF FIGURES	IX
ABBREVIATIONS	X
CHAPTER 1: INTRODUCTION	1
1.1. Introduction	1
1.2. Wetland Ecosystem Services.....	2
1.3. Objectives.....	3
1.4. Study Site.....	4
1.5. Previous Research on Prescribed Fire Effects to Wetlands.....	5
1.6. References.....	8
CHAPTER 2: LITERATURE REVIEW-PRESCRIBED FIRE AND SOIL MOISTURE DYNAMICS.....	10
2.1. Introduction	10
2.2. Approaches to Determine Hydrophobicity.....	11
2.2.1. Water Droplet Penetration Time Test (WDPT)	11
2.2.2. Capillary Rise Method (CRM)	11
2.2.3. Molarity of an Ethanol Droplet Test (MED).....	12
2.2.4. Du Noüy Ring Tensiometer.....	12
2.2.5. Minidisk Infiltrometer.....	13
2.3. Prescribed Fires Effect on Hydrophobicity.....	14
2.4. Approaches Used to Evaluate Hydraulic Conductivity.....	17
2.4.1. Saturated Hydraulic Conductivity.....	17
2.4.2. Unsaturated Hydraulic Conductivity.....	18
2.5. Effect of Prescribed Fires on Hydraulic Conductivity.....	19
2.6. Conclusion.....	22
2.7. References.....	23
CHAPTER 3: PRESCRIBED FIRE EFFECTS ON SOIL PROPERTIES AND NUTRIENT DYNAMICS IN A FORESTED WATERSHED.....	27
3.1. Abstract.....	27
3.2. Introduction.....	28
3.3. Methods.....	31
3.3.1. Soil Infiltration Sampling.....	35
3.3.2. Soil Laboratory Analysis.....	36
3.3.3. Statistical Analysis.....	37
3.4. Results.....	38
3.4.1. Soil Bulk Density and Texture	38
3.4.2. Unsaturated Hydraulic Conductivity and Water Repellency	39
3.4.3. Nutrient Content.....	40
3.4.4. Carbon and Nitrogen Isotopic Ratios.....	43

3.5. Discussion.....	45
3.5.1. Soil Properties.....	45
3.5.2. Hydrological Properties.....	46
3.5.3. Nutrient Concentrations.....	47
3.5.4. Carbon and Nitrogen Isotopic Ratios Alterations.....	50
3.6. Conclusion.....	52
3.7. References	55
APPENDIX A: SOIL PROPERTIES.....	61
A.1. Soil Descriptions.....	61
A.2. Bulk Density.....	67
A.3. Grain Size Analysis.....	68
APPENDIX B: HYDROLOGICAL PROPERTIES.....	76
B.1. Water Infiltration Raw Data.....	77
B.2. Ethanol Infiltration Raw Data.....	80
B3. Statistical Analysis.....	83
APPENDIX C: NUTRIENTS.....	85
C.1. Statistical Analysis.....	85
APPENDIX D: CARBON AND NITROGEN ISOTOPIC RATIOS.....	92
D.1. Carbon and Nitrogen Isotopic Ratios Raw Data.....	92
D.2. Statistical Analysis.....	93

CHAPTER 1: INTRODUCTION

1.1. Introduction

In the United States, forests cover an estimated 21.73 square kilometers of a total wetland area (Bridgham et al. 2006). Modern prescribed fire practices are a primary management tool used to reduce the likelihood of wildfire events, pathogens, overgrowth, and overpopulation of foliage communities (Boring et al. 2004; Richter et al. 1982, Mitchell et al. 2014). Prescribed fires are applied to a forest when fuel and soil moisture levels are either normal or high so that only the forest understory is burned (Carter and Foster 2004). Because less than 50% of litter available on the forest floor is consumed in any given burn and there are fewer nutrients released, this separates them from wildfires (Carter and Foster 2004).

When compared to the rest of the United States, 2/3 of the areas that are burned in the South are due to prescribed fires and not wildfires (Figure 1). Specifically in the Southeast, forests have been undergoing prescribed fire regimes for more than 10,000 years (Fowler and Konopik 2007). Because the Southeastern US is composed of young forests, making them ideal for nutrient sequestration due to the aggradation, or build-up of sediments, and high level of net primary productivity, it is important to understand the environmental implications associated with this essential land management tool (Mitchell et al. 2014). A variety of studies have looked at the overall effects of wildfires in the western US, but few have investigated the effects of prescribed fires on nutrient cycling in the south with the emphasis being to forested wetland regions.

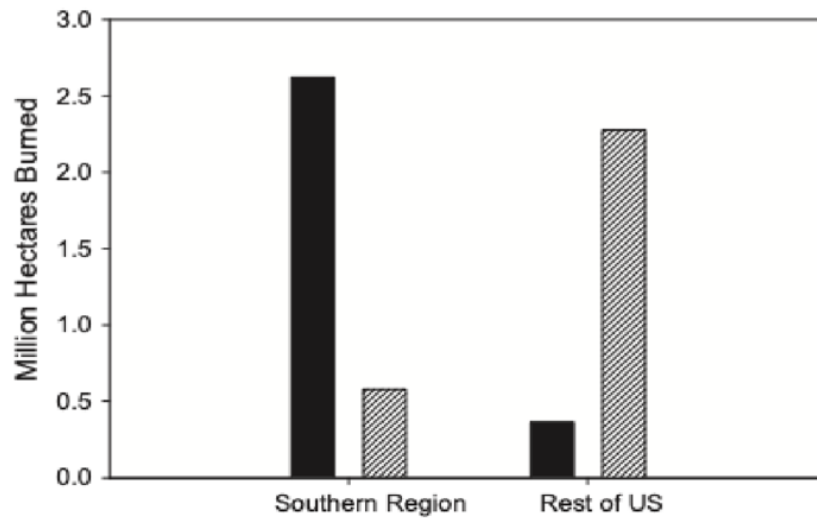


Figure 1. Prescribed fire-affected areas (solid bars) and wildfire areas (hatched bars) within the United States investigated in 2011 (Mitchell et al. 2014).

1.2. Wetland Ecosystem Services

Wetland regions have a biogeochemical function that aids in carbon sequestration, sediment trapping, and uptake of nutrients, all of which are ecosystem services (Marton et al. 2015). The anoxic conditions in wetlands are ideal because when oxygen is removed from a system, this enables microbial processes to slow down and allow nutrients to accumulate and be stored. Because of the redox conditions in wetlands, this helps protect aquatic environments by retaining and preventing the transport of solutes, chemicals, and nutrients from reaching into downstream aquatic ecosystems (Marton et al. 2015). Although wetlands are ideal for nutrient storage, they can also influence the release of gases into the atmosphere. For example, anoxic soils in wetlands are ideal for denitrification processes which promotes the release of nitrogen gas (Racchetti et al. 2011). Currently, due to the ecosystem services, wetlands, with the exception of geographically isolated wetlands, that are connected to navigable surface waters, are being protected under the Clean Water Act (Marton et al. 2015).

Geographically isolated wetlands (GWIs) are referred to as being “isolated” because they are surrounded by upland regions (Marton et al. 2015). These wetlands are naturally created as depressions in the landscape that accumulate rainfall, which aids in maintaining soil saturation, and retaining nutrients in sediments, all of which supports hydrophytic vegetation and organisms in the area (Marton et al. 2015). Despite the lack of hydrological connectivity to nearby open water bodies, geographically isolated wetlands still have hydrological, ecological, and chemical connectivity to the broader landscapes that can provide ecosystem services, which is why they are worth investigating. Numerous research has evaluated the effects of prescribed fire on longleaf pine stands broadly both internationally (Näthe et al. 2018; Fernández et al. 1997; Blake et al. 2010) and in the US (Lavoie et al. 2010; Boring et al. 2004; Carter and Foster 2004), but few have focused on the effects within forested geographically isolated wetland sites. It is important to document how these unique systems respond to prescribed fire.

1.3. Objectives

The purpose of this study is to determine the short-term (immediate) and long-term (chronic) effects prescribed fires have on nutrient cycling in a longleaf pine forested geographically isolated wetland region. By comparing two wetlands and their surrounding uplands, with one representing immediate (burned over a 2-month interval) and the other demonstrating chronic (one-year post-fire) effects, I will determine to what extent does fire affect soil moisture dynamics, specifically unsaturated hydraulic conductivity and water repellency, soil texture, nutrients, and carbon and nitrogen isotopic ratios. Using two-way ANOVA analyses and unpaired t-tests, paired by sampling locations, I will focus on alterations to nutrient dynamics, soil texture, as well as carbon and nitrogen isotopic ratio signatures in surface and subsurface soil horizons along a low-relief hillslope. An unpaired t-test will also be utilized to

determine changes to soil moisture dynamics. By performing a principal component analysis, similar ordination of nutrients will be represented in respect to pre-fire and post-fire conditions in the experimental site. These different data sets will serve to evaluate (1) fire-induced changes to soil moisture dynamics deriving from the surface horizon (2) whether or not prescribed fire can change nutrient movement with depth in a soil profile and (3) the effects prescribed fire will have on nutrient content and carbon and nitrogen isotopic signatures in surface and subsurface horizons.

1.4. Study Site

The study site is a longleaf pine forest with geographically isolated wetlands (GIW) located at the Jones Center at Ichauway, a private research center, in Baker County, Georgia (Figure 2). In this study, I used two GIW sites, which are reference sites for a larger collaborative project investigating the temporal and spatial variability of nutrient processes in an agricultural ecosystem. Although these sites have not been altered by modern agricultural production, they have experienced frequent rotational prescribed burning for more than 10 years, making them ideal sites for this study.

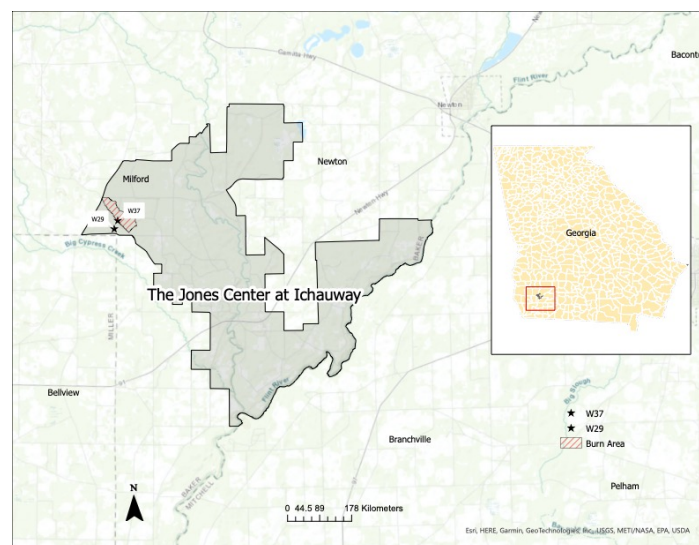


Figure 2. Study site at the Jones Center at Ichauway in Georgia, USA.

1.5. Previous Research on Prescribed Fire Effects to Wetlands

Because forested areas are managed with prescribed fires in geographically isolated wetlands, it is important to understand the allochthonous contributions this forest management practice has within these watersheds. Although prescribed fires are low in intensity, they have the potential to change soil characteristics, which can impact soil stability, soil aggregates, and hydrological properties (Shakesby and Doerr 2006). For example, fire in general, has been shown to influence soil erosion, which can alter sediment composition and transport. It has been mentioned that prescribed fires could increase sediment yield, but it all depends on the severity of the fire (Scott and Van Wyk 1990). In one study, rainfall simulations and infiltration experiments for different burn severities were used to study wildfire effects to hydrology, soil erosion, sediment yield, and phosphorus concentrations along a hillslope (Blake et al. 2010). Water and sediments samples were collected and analyzed for phosphorus contents in a hillslope after a 20, 40, and 60 mm h⁻¹ rainfall simulation event (Blake et al. 2010). They found that in hillslopes that were burned severely, sediment yield, dissolved inorganic phosphorus, and particulate phosphorus concentrations were high in eroded sediments (Blake et al. 2010). Because particulate phosphorus yield was higher than dissolved inorganic phosphorus yield, this indicated that sediments are the vectors that facilitate nutrient movement in a watershed basin (Blake et al. 2010). This was significant because after an intense rainfall and severe fire, a hillslope can be susceptible to erosion causing the sediment and phosphorus transport to increase downslope, which could be detrimental to nearby aquatic systems (Blake et al. 2010). Although this study focused on wildfires effects to phosphorus concentrations, it will be interesting to see if prescribed fires could affect the movement of other elements as well. Because sediments are an integration of different components, they have a role in nutrient storage and can signalize

landscape processes in a wetland basin. In general, if fire has the potential to alter soil structure, movement, and hydrological properties, low-intensity fires can potentially change biogeochemical functions in a wetland basin.

Research has shown that fire events can affect the biogeochemical processes of a forested watershed by releasing nutrients from the forest floor into either the atmosphere, nearby fluvial systems, or into other areas in close proximity (Richter et al. 1982). Studies have documented changes in water quality and gas emission resulting from an applied burn. For example, Battle and Golladay (2003) has shown the effects prescribed fires have on water quality where there was an increase in pH, bioavailable phosphorous, dissolved organic carbon, alkalinity, and ammonium in water samples exposed to fire treated soils (Battle and Golladay 2003). Akagi et al. (2014) also showed prescribed fires influencing the release of trace gases which can have health implications (Akagi et al. 2014).

Few studies have recorded changes to nutrient cycling in wetland soils after a fire. In one study, researchers investigated the effects of prescribed fire on nutrient availability and the importance of the changes in a bog ecosystem (Wilbur and Christensen 1983). They found that after a fire there was an increase in available K, PO₄-P, Mg, NO₃-N, and NH₄-N but only PO₄-P and NO₃-N showed a difference in spatiality where it could potentially lead to the creation of nutrient patches (Wilbur and Christensen 1983). In another study, nutrient alterations and gas emissions were investigated in marsh ecosystems one year after a prescribed burn (Schmalzer and Hinckle 1992). Nitric oxide and methane were also of focus in this research. In burned marshes, they found that pH increased post-fire and eventually returned to pre-fire conditions one month after the event. In the upper horizon, they found an increase in organic matter content and observed burned residue in the waterbody of the marsh (Schmalzer and Hinckle 1992). The

nutrients Ca, Mg, and K increased a month post-fire and researchers attributed such change in the soil to the release of the cations from the burning of biomass. Because conductivity increased as well, they stated that burned biomass and ash could cause cations to increase. It was also mentioned that a month, after the prescribed fire occurrence, PO₄-P and NH₄-N increased as well (Schmalzer and Hinckle 1992). Overall, if prescribed fires have the ability to alter natural biogeochemical cycling in a wetland basin, this can affect nutrient availability, transport, and sequestration.

1.6. References

- Akagi, S.K., Burling, I.R., Mendoza, A., Johnson, T.J., Cameron, M., Griffith, D.W.T., Paton-Walsh, C., Weise, D.R., Reardon, J., and Yokelson, R.J., 2014, Field measurements of trace gases emitted by prescribed fires in southeastern US pine forests using an open-path FTIR system, *Atmospheric Chemistry and Physics*, v. 14, no. 1, p. 199-215.
- Battle, J., and Golladay, S.W., 2003, Prescribed fire's impact on water quality of depressional wetlands in southwestern Georgia, v.150, no.1, p. 15-25.
- Blake, W.H., Theocharopoulos, S.P., Skoulikidis, N., Clark P., Tountas, P., Hartley R., Amaxidis Y., 2010, *Journal of Soils and Sediments*, v. 10, p. 671–682, DOI 10.1007/s11368-010-0201-y
- Boring, L.R., Hendricks, J.J., Wilson, C.A., and Mitchell R.J., 2004, Season of burn and nutrient losses in a longleaf pine ecosystem, *International Journal of Wildland Fire*, v.13, p. 443–453, doi:10.1071/WF03060
- Bridgham, S.D., Megonigal, J.P., Keller, J.K., Bliss N.B., Trettin C., 2006, The carbon balance of North American wetlands, *Wetlands* no. 26, v. 4, p. 889–916.
- Carter, M.C. and Darwin Foster, C., 2004, Prescribed burning and productivity in southern pine forests: a review, *Forest Ecology and Management*, v. 191, p. 93–109, doi:10.1016/j.foreco.2003.11.006
- Fernández, I., Cabaneiro, A., and Carballas, T., 1997, Organic matter changes immediately after a wildfire in an Atlantic forest soil and comparison with laboratory soil heating, *Soil Biology and Biochemistry*, v. 29, p. 1–11.
- Fowler, C., and Konopik, E., 2007, The history of fire in the southern United States, *Human Ecology Review*, v. 14, no.2, p. 165-176.
- Lavoie, M., Starr, G., Mack, MC., Martin, T.A., and Gholz, H.L., 2010, Effects of a prescribed fire on understory vegetation, carbon pools, and soil nutrients in a longleaf pine-slash pine forest in Florida, v. 30, no. 1, *Natural Areas Journal*, p. 82-94.
- Marton, J. M., Creed, I. F., Lewis, D. B., Lane, C. R., Basu, N. B., Cohen, M. J., and Craft, C. B., 2015, Geographically isolated wetlands are important biogeochemical reactors on the landscape, *Bioscience*, no. 65, v. 4, p. 408–418.
- Mitchell, R.J., Liu, Y., O'Brien J.J., Elliott K.J., Starr G., Miniati C.F., and Hiers J.K., 2014, Future climate and fire interactions in the southeastern region of the United States, *Forest Ecology and Management*, p. 1-11.

- Näthe, K., Levia, D.F., Tischer, A., and Michalzik, B., 2018, Low-intensity surface fire effects on carbon and nitrogen cycling in soil and soil solution of a Scots pine forest in central Germany, *Catena*, v. 162, p. 360-375.
- Racchetti, E., Bartoli, M., Soana, E., Longhi, D., Christian, R.R., Pinardi, M., Viaroli, P., 2011, Influence of hydrological connectivity of riverine wetlands on nitrogen removal via denitrification, *Biogeochemistry*, v. 103, p. 335–354.
- Richter, D. D., Ralston, C. W., and Harms W.R., 1982, Prescribed Fire: effects on water quality and forest nutrient cycling, *Science*, v. 215, no. 4533, p. 661-663.
- Schmalzer, P.A., and Hinkle, C.R., 1992, Soil dynamics following fire in *Juncus* and *Spartina* marshes., *Wetlands*, v. 12., no.1, p.8-21.
- Scott, D.F., and Van Wyk, D.B., 1990, The effects of wildfire on soil wettability and hydrological behaviour of an afforested catchment. *Journal of Hydrology*, v. 121, p. 239–256.
- Shakesby, R.A., and Doerr, S.H., 2006, Wildfire as a hydrological and geomorphological agent, *Earth Science Reviews*, v. 74, p. 269-307.
- Wilbur, R.B., and Christensen, N.L., 1983, Effects of fire on nutrient availability in a North Carolina coastal plain pocosin, *The American Midland Naturalist*, v. 110, no.1, p. 54-61.

CHAPTER 2: LITERATURE REVIEW- PRESCRIBED FIRE AND SOIL MOISTURE DYNAMICS

2.1. Introduction

Studies have shown that fire can impact soil stability and porosity which can alter water infiltration (Shakesby and Doerr 2006). As fire changes soil properties, soil structure, and vegetation this, in turn, affects the hydrological and geomorphological processes in the landscape (Shakesby and Doerr 2006). As these three different components are modified, this can then influence infiltration rate, overland flow, and detachment of soil particles (Shakesby and Doerr 2006).

Under natural conditions, hydrophobicity in the soil can be caused by multiple factors deriving from water-repellent compounds originating from root systems, formed as a byproduct from fungal or microbial communities, or generated as organic matter decays (Dekker and Ritsema 1996; Doerr 1998; McGhie and Posner 1981, Doerr et al. 2005). As fire consumes more organic matter, this can cause the soil structure to collapse making the soil denser (Neary et al. 2005). As soil structure changes, this can affect water infiltration which changes hydraulic conductivity. It is said that when soil moisture surpasses 12-25%, hydrophobicity is not present in the soil (Huffman et al. 2001).

Because soil moisture content varies, hydrophobicity and hydraulic conductivity have an inverse relationship which can potentially alter the transport of water-soluble elements as water infiltrates and percolates within a soil profile. Due to potential implications in nutrient transport, it is imperative we understand the effects associated with fire-induced alterations to soil moisture dynamics. In this literature review, we will focus on the direct effects prescribed fire has on hydraulic conductivity and water repellency. Mathematical models used to quantify and measure

soil hydrophobicity and hydraulic conductivity will be discussed as well as research studies that investigated prescribed fire effects.

2.2. Approaches to Determine Hydrophobicity

2.2.1. Water Droplet Penetration Time Test (WDPT)

One of the most common techniques developed to test for hydrophobicity in the soil is referred to as the Water Droplet Penetration Time (WDPT) where a drop of water is initially placed on the soil and then the time it takes for the drop to infiltrate within the surface is recorded (Olorunfemi et al. 2014). The time it takes for the drop to penetrate in the soil can determine the strength of the hydrophobicity. Researchers have developed different classifications using this method but there are limitations because other factors such as surface roughness can affect measurements (Olorunfemi et al. 2014). This technique is effective in that it can help indicate the hydrological effects of hydrophobicity (Doerr 1998; Leelamanie et al. 2008).

2.2.2. Capillary Rise Method (CRM)

The Capillary Rise technique is used to determine the contact between a liquid and a solid (Olorunfemi et al. 2014). This test is utilized to evaluate the capillary rise on a liquid in an unsaturated column containing either powder or more granular matter (Letey et al. 1962; Leelamanie et al. 2008). The contact angle can be determined with the use of the equation (Washburn 1921; Leelamanie et al. 2008; Olorunfemi et al. 2014):

$$Y = \Delta pghr/2 \cos \theta \quad (\text{Equation 1})$$

Where p is represented as the liquid's density, g is gravity, h is the height of the capillary rise, r is the pore radius, and θ is the angle of the contact between a liquid and a solid (also referred to as the wetting angle) (Olorunfemi et al. 2014).

2.2.3. Molarity of an Ethanol Droplet Test (MED)

The molarity of an Ethanol Droplet test (MED) measures what the molarity of an ethanol droplet is needed to record infiltration in the soil surface (Olorunfemi et al. 2014). Different ethanol concentrations are used to modify the tension of the liquid's surface. Water repellency can be inferred from this tool where the least concentration of ethanol adsorption that can enable infiltration of a water drop is determined (Olorunfemi et al. 2014). The surface tension can be recorded by increasing ethanol concentration which can allow researchers to determine the strength of the repellence of the water in the soil. It has been mentioned that this method can poorly indicate infiltration rates in the soil (Olorunfemi et al. 2014).

2.2.4. Du Noüy Ring Tensiometer

An instrument is used to measure the surface and interfacial tension where a platinum ring is placed in a test liquid to determine repellency (Olorunfemi et al. 2014). This method can help evaluate the surface and interfacial tension at distinct interfaces whether it be liquid to liquid or air to liquid. The force required to extract the platinum ring from the liquid test can be calculated using the equation:

$$\gamma = \frac{F}{P \cos \theta} f \quad (\text{Equation 2})$$

Where γ is, the total force needed, P is the saturated perimeter of the three-phase contact, θ is the contact angle recorded from the contact from the meniscus of the liquid to the surface of the object, f is represented as the correction factor that can range from 0.75-1.05, and F is the force (Olorunfemi et al. 2014).

2.2.5. Minidisk Infiltrometer

A minidisk infiltrometer apparatus has also been used to evaluate infiltration in the soil where two different liquids are used to assess changes (Olorunfemi et al. 2014, Figure 1). In this apparatus, the top chamber, or Mariotte chamber, is filled with water, while the bottom chamber, or reservoir, is filled with 95% ethanol (Lichner et al. 2007). Using the suction control tube, the suction rate is set to 2 cm. After this setup, the researcher can select a designated timing interval to determine ethanol infiltration in the soil (METER 2021). The timing it takes for the ethanol to infiltrate the soil surface can be indicative of the presence of hydrophobicity (Lichner et al. 2007) (METER 2021).

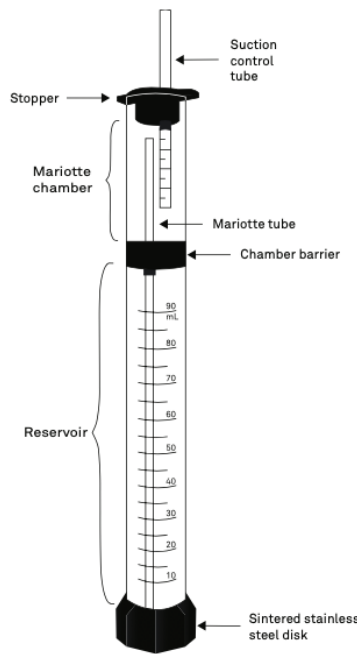


Figure 1. Minidisk infiltrometer apparatus (METER 2021)

In order to determine soil water repellency, the slope of the cumulative infiltration can be calculated using the formula (METER 2021):

$$I = S_e \sqrt{t} \quad (\text{Equation 3})$$

Where I is the cumulative infiltration, S_e is ethanol sorptivity, and t is the square root of time in seconds. The slope of the water sorptivity can be calculated using the expression (METER 2021):

$$I = S_w \sqrt{t} \quad (\text{Equation 4})$$

Where I is infiltration, S_w is water absorptivity, and t is the square root of time recorded in seconds. Once the slope of both ethanol and water sorptivity are calculated, hydrophobicity can be determined using the repellency index equation (Hallett et al. 2001):

$$R = 1.95 ((S_{ethanol}) / (S_{water})) \quad (\text{Equation 5})$$

Where R is the repellency index, $S_{ethanol}$ is the slope of the ethanol sorptivity, and S_{water} is the slope of the water sorptivity.

2.3. Prescribed Fires Effect on Hydrophobicity

Fire induced soil water repellency can leave an area vulnerable to erosion, by increasing erosive energy in a given hillslope which can potentially create overland flow (Scott and Van Wyk 1990). Hydrophobicity is difficult to isolate due to its relationship with soil moisture, organic matter content, hydraulic conductivity, air permeability, and other such parameters, but studies have attempted to investigate its persistence in a region where changes are contingent on fire intensity, fire duration, and soil type. The repellency in the soil is dependent upon the time since the initial burn, but the effects of water repellency typically weaken after a period of three months (Macdonald and Huffman 2004). Fire that burns over 20 minutes, with temperature ranges between 800-900 degrees, can potentially destroy non-wettable property in soil, but there is still uncertainty when it comes to measuring water repellency (Debano and Krames 1966).

Some studies have shown that water repellency can reduce infiltration in the soil, while others mention the contrary (Debano and Krames 1966).

In one study, researchers studied the effects of wildfire and prescribed fires on soil hydrophobicity in a ponderosa and lodgepole pine forests (Huffman et al. 2001). Researchers were interested in investigating the effects that time, burn intensity, vegetation, soil type, and soil moisture has on soil water repellency after an initial burn. Soil water repellency was determined by using the water drop penetration time technique and the critical surface tension measurements at different soil depths. They found that at sites that experienced moderately to severe fire, there was strong soil hydrophobicity at the soil depth of 0, 3, and 6 centimeters. On the other hand, sites that were burned at low severity, which is similar in scale to prescribed fires, were repellent on the surface only. Soil water repellency seemed to increase with increasing fire intensity, but because there was such variability in between study sites, it was difficult to determine if there were significant statistical differences (Huffman et al. 2001). They determined that although hydrophobicity was not present when soil moisture was high, it persisted in the area the more sand content there was in the soil. After 3 months, soil hydrophobicity decreased but was still present in the soil for about 22 months. Researchers mentioned that prescribed fires can cause strong water repellency in soil if there is a higher fuel load. If there is higher fuel load in an area, this could potentially impact the depth and durability of the soil water repellent layer in the soil. Researchers mentioned that the effects of soil moisture on soil water repellency could be further investigated in the future by determining if there exists a threshold for saturation in hydrophobic soils. In the future, they recommended that critical surface tension measurements were better at determining hydrophobicity than water drop penetration time measurements because it was easier to calculate and had less variability (Huffman et al. 2001).

In another study, water repellency was measured by using the water drop penetration time method in a shrubland before and after fire events (Stoof et al. 2011). They were interested in determining to what extent did fire affect hydrophobicity and whether or not soil moisture was the main driver for differences in soil water repellency. They also investigated the effects organic matter content has on soil water repellency. Researchers found that surface water repellency was influenced by soil moisture in samples. There was a negative correlation found where soil water repellency tended to increase as soil moisture decreased. They also found that in severely to extremely repellent samples, soil water repellency increased with organic matter composition. Saturated soil samples had greater organic matter content than slightly to severely repellent samples (Stoof et al. 2011). This difference could be attributed to the greater moisture content present in wet soil samples where organic matter could potentially increase water retention in soil. Fire increased the water drop penetration time in the samples, or commonly referred to as persistence of soil water repellency, in this study but did not significantly impact soil moisture content in the soil. After a fire, hydrophobicity in the soil appeared rapidly, but disappeared in a span of 4 days due to continuous rainfall in the samples collected. In a fire affected area, soil water repellency disappeared faster than in an unburned site. Both, vegetation removal and fire, minimized the time and precipitation required to remove hydrophobicity in soil and foliage litter from an initial rainfall of about 650 mm in a time period of 75 days to 30-50 mm in 4 to 6 days. Researchers concluded that soil water repellency is influenced by both soil moisture and organic matter content, which can affect hydrological processes (Stoof et al. 2011).

Overall, it is difficult to address water repellency because not only does fire affect regions differently, but it is hard to isolate it from other hydrological parameters (Doerr et al. 2003). The studies mentioned have attempted to investigate the parameters used to determine the

impacts of repellency where severity, spatial distribution, transient characteristics, and character and spatial distribution of routeways and wettable subsoil are variable factors. It is important to study the effects of all these different parameters because a change in one factor can potentially impact other variables (Doerr et al. 2003). Although it is hard to isolate hydrophobicity, it will impact soil type differently.

2.4. Approaches Used to Evaluate Hydraulic Conductivity

2.4.1. Saturated Hydraulic Conductivity

The study of water movement through a porous media was first applied by Henry Darcy where he helped experimentally design the methodology to evaluate hydraulic conductivity (Darcy 1856; Zhang and Schaap 2019). Hydraulic conductivity or the coefficient of permeability can be calculated by using the formula of Darcy's law that indicates:

$$K = -Q/A(dh/dl) \quad (\text{Equation 6})$$

Where K is hydraulic conductivity, Q is discharge, A is cross-sectional area, and dh/dl is the hydraulic gradient. This formula has been altered by Hubbert 1956 where he discussed that K is a function of porous medium and the fluid (Hubbert 1956; Fetter 2001). Hydraulic conductivity of sandy sediments has also been discussed where K is related to the square of an attribute dimension of a sediment (Hazen 1911; Fetter 2001). Another study has also evaluated hydraulic conductivity and connected it to grain size (Shepherd 1989; Fetter 2001).

The Kozeny-Carman equation has also been used in different studies to evaluate changes to hydraulic conductivity by means of permeability referred to as intrinsic permeability with the use of the formula (Zhang and Schaap 2019):

$$K = \phi RH^2/GT^2 \quad (\text{Equation 7})$$

Where K is hydraulic conductivity, ϕ is porosity, RH is hydraulic radius, G is the pore shape factor, and T is tortuosity. Another study has also represented the Kozeny-Carman equation to be (Glatstein and Francisca 2014; Zhang and Schaap 2019):

$$K = (pg/\mu)l/K^*T^2S_0^2(e^3/1+e)S^3 \quad (\text{Equation 8})$$

Where K is hydraulic conductivity, p is the density of the fluid, g is gravitational acceleration, μ is viscosity of the fluid, T is tortuosity, K^* is the pore shape factor, S_0 is the wetted surface area per unit volume, e is the ratio of the void, and S is the saturation degree.

2.4.2. Unsaturated Hydraulic Conductivity

Gravity potential and moisture potential are used to determine water infiltration in the unsaturated zone giving segue to the theory of unsaturated flow (Childs 1967; Fetter 2001). Darcy's law is still applicable when discussing unsaturated flow thus introducing the concept of unsaturated hydraulic conductivity. In unsaturated soil, soil moisture moves downward in water-filled pores where there can be air as well (Fetter 2001). As water content increases, more pores can retain water which will eventually increase the downward movement of water. Unsaturated hydraulic conductivity is determined as being the function of volumetric water content whereas it increases, unsaturated hydraulic conductivity increases as well (Fetter 2001). This relationship regarding volumetric water content and moisture potential is currently expressed using Richard's Equation (Varado et al. 2006):

$$\frac{\partial \theta}{\partial t} = \frac{\partial}{\partial z} \left[K(h) \left(\frac{\partial h}{\partial z} - 1 \right) \right] \quad (\text{Equation 9})$$

Where K is hydraulic conductivity, h is the pressure head, θ is volumetric water content, z is the depth, and t is the time.

With the use of minidisk infiltrometer, an effective method was also developed to measure sorptivity of water and unsaturated hydraulic conductivity expressed as (Lichner et al. 2007; Zhang 1997):

$$I=C_1(h_0)t^{1/2} +C_2 (h_0)t \quad (\text{Equation 10})$$

Where I is infiltration, h_0 represents pressure head, $C_1(h_0)$, and $C_2 (h_0)$ are indicative of pressure head functions while unsaturated hydraulic conductivity is expressed as (Lichner et al. 2007; Zhang 1997):

$$K(h_0)=C_2(h_0)/A_I \quad (\text{Equation 11})$$

Where unsaturated hydraulic conductivity is represented as $K(h_0)$, $C_2 (h_0)$ is a function of the pressure head, and A_I is a constant.

2.5. Effect of Prescribed Fires on Unsaturated Hydraulic Conductivity

Calculations derived from the moisture retention curve has been effective in determining fire-induced changes to hydrological properties, but such method has biases incorporated and is normally utilized in spatial studies (Vogel and Cislerova 1988). Rainfall model simulations are used to determine unsaturated hydraulic conductivity where the difference between precipitation and runoff are computed (Robichaud 2000; Kennard and Gholz 2001; Savadogo et al. 2007; Plaza-Alvarez et al. 2018; Rau et al. 2005). Although indirect methods have been demonstrated to be more practical, there have been few studies that have investigated changes to hydraulic conductivity directly with the use of an infiltrometer.

In one study, researchers used an air permeameter and a minidisk tension infiltrometer to determine the effects a single low intensity prescribed fire has on near-saturated hydraulic conductivity, air permeability, and physical soil properties under canopy and interspaced microsites before and after fire treatment in a semiarid shrub woodland transition zone region

(Chief et al. 2012). Using the measurements collected, they were interested in determining the impacts that the fire-affected soil structure has on hydraulic properties (Chief et al. 2012). They determined that in situ air permeability increased from 21% to 37% post-fire in both under canopy and interspace microsities, however this was not statistically significant. Researchers found that water repellency did not change near-saturated hydraulic conductivity in under canopy microsities and was absent in interspace microsities (Chief et al. 2012). This could have been due to the expansion of water as it vaporized through the soil pores as soil structure collapsed (Chief et al. 2012). Because prescribed fires are small-scale and low in intensity, surface temperature was not high enough to volatilize organic matter and change physical soil properties within interspace microsities. They determined that this could be due to heat transfer and water vaporization, which eventually caused soil structure to collapse as soil pores expanded (Chief et al. 2012). Based on their findings, they concluded that after a fire, changes to soil structure had a greater impact on soil hydrology and physical soil properties than soil water repellency alone (Chief et al. 2012).

In another study, the effects of fire frequencies on soil hydrological properties were investigated where they looked at the changes to saturated and unsaturated hydraulic conductivity in a Savanna (Strydom et al. 2019). A tension disc infiltrometer was used to assess such changes. They found that frequent annual fires did not reduce unsaturated hydraulic conductivity when compared to unburned sites where fire has not been used as a management tool in the last 60 years since the study took place (Strydom et al. 2019). They determined that there was a significant difference in the rates of unsaturated hydraulic conductivity in between the various fire frequencies on soils where the dominant parent material was granite (Strydom et al. 2019). Unsaturated hydraulic conductivity was lower on the granite burned plot when

compared to the unburned plot. In soils where the parent material was dominantly granite and basalt, fire did not significantly affect saturated hydraulic conductivity (Strydom et al. 2019). Researchers discussed that there was an apparent strong positive correlation between unsaturated hydraulic conductivity and the time after a fire in granite plots (Strydom et al. 2019).

In a study, researchers were interested in determining the effects prescribed fire has on infiltration in the soil in Mediterranean forests (Plaza-Alvarez et al. 2019). A minidisk infiltrometer was used to determine hydraulic conductivity. It was found that prescribed fire did not affect unsaturated hydraulic conductivity significantly (Plaza-Alvarez et al. 2019). There was no relationship nor pattern found between hydraulic conductivity, prescribed fire, treatment nor with time after the fire. It was concluded that fire intensity could have impacted their results causing there to be no significant changes resulting from the treatment (Plaza-Alvarez et al. 2019).

In West Africa, researchers investigated the effects prescribed fires and grazing intensification had on infiltration, vegetation cover, and forage productivity (Savadogo et al. 2007). Double ring infiltrometers were used in this study to determine the effects. It was found that prescribed fire impacted steady state infiltration where there was a decrease in infiltrability. Researchers discussed that they were unable to control fire intensity which can have varying impacts on soil properties (Savadogo et al. 2007).

Indirect methods are commonly utilized to determine the spatial impacts prescribed fires have on hydrological properties, but direct measurements can demonstrate potential temporal effects. It is crucial that potential temporal effects are taken into consideration because there can be variable changes in ecosystems according to different soil textures. Relying on indirect approaches creates generalizations and can underestimate or overestimate effects. If temporal

effects of prescribes to hydraulic conductivity are further evaluated, this can help create more accurate simulation models in the future.

2.6. Conclusion

Prescribed fires are beneficial in the creation of a diverse mosaic forest community, but there is a research gap in addressing the connection between the short-term effects of prescribed fire on soil moisture dynamics and nutrient movement in sediment soils according to specific biomes. Although direct methods take time and are not as feasible, they can help quantify the temporal effects to hydrological properties. Investigating temporal changes to water infiltration can aid in the development of more accurate models to improve forest management. Decreasing the potential biases of models, can help inform how we adapt our forest management practices in response to climate change to better protect ecosystem services.

2.7. References

- Chief, K., Young, M.H., and Shafer, D.S., 2012, Changes in soil structure and hydraulic properties in a wooded-shrubland ecosystem following a prescribed fire, *Soil Science Society of America Journal*, p. 1965-1977.
- Childs, E.C., 1967, Soil Moisture Theory, In *Advances in Hydrosience*, v. 4., ed. V.T. Chow., 73-117, New York: Academic Press.
- Darcy, H.P.G., 1856, *Les Fontaines publiques de la ville de Dijon*. Paris: Victor Dalmont.
- DeBano, L.F., and Krammes, J.S., 1966, Water repellent soils and their relation to wildfire temperatures, *International Association of Scientific Hydrology, Bulletin*. no. 11, p. 14–19, doi:10.1080/02626666609493457
- Dekker, L.W., Ritsema, C.J., 1996, Variation in water content and wetting patterns in Dutch water repellent peaty clay and clayey peat soils, *Catena*, v. 28, p. 89–105, doi: 10.1016/S0341-8162(96)00047-1
- Doerr, S.H., 1998, On standardizing the ‘water drop penetration time’ and the ‘molarity of an ethanol droplet’ techniques to classify soil hydrophobicity: A case study using medium textured soils, *Earth Surface Processes Landforms*, v. 23, p. 663– 668.
- Doerr, S.H., Ferreira, A.J., Walsh, R.P.D., Shakesby, R.A., Leighton-Boyce, G., and Coelho C.O.A., 2003, Soil water repellency as a potential parameter in rainfall–runoff modelling: Experimental evidence at point to catchment scales from Portugal, *Hydrological Processes*, v. 17, p. 363–377, doi:10.1002/hyp.1129
- Doerr, S.H., Llewellyn, C.T., Douglas, P., Morley, C. P., Mainwaring, K. A., Haskins, C., Johnsey L., Ritsema, C. J., Stagnitti, F., Allinson, G., Ferreira, A. J. D., Keizer, J. J., Ziogas, A. K., Diamantis, J., 2005: Extraction of compounds associated with water repellency in sandy soils of different origin, *Australian Journal of Soil Research*, v. 43, p. 225–237.
- Fetter, C.W., 2001, *Applied Hydrogeology*, 4th edition, Waveland Press, Inc., Long Grove, Illinois.
- Glatstein, D.A., and Francisca F.M., 2014, Hydraulic conductivity of compacted soils controlled by microbial activity, *Environmental Technology*, v. 35, no.15, p.1886-1892.
- Hallett, P.D., Baumgartl, T., and Young, I.M., 2001, Subcritical water repellency of aggregates from a range of soil management practices, *Soil Science Society of America Journal*, v. 65, p. 184–190.
- Hazen, A., 1911, Discussion: dams on sand foundations, *Transactions of the American Society of Civil Engineers*, v. 73, p.199-203.

- Hubbert, M.K., 1956, Darcy's Law and the Field Equations of flow of underground fluids. Transactions, American Institute of Mining and Metallurgical Engineers, v. 207, p. 222-39.
- Huffman, E.L., MacDonald, L.H., and Stednick, J.D., 2001, Strength and persistence of fire-induced soil hydrophobicity under ponderosa and lodgepole pine, Colorado Front Range, Hydrological Processes, v. 15, p. 2877–2892, doi:10.1002/hyp.379
- Kennard, D.K., Gholz, H., 2001, Effects of high-and low-intensity fires on soil properties and plant growth in a Bolivian dry forest, Plant Soil, v. 234, p. 119–129.
- Leelamanie, D. A. L., Karube, J., and Yoshida, A., 2008, Characterizing water repellency indices: contact angle and water drop penetration time of hydrophobized sand, Soil Science and Plant Nutrition, v. 54, no.2, p. 179-187, DOI: 10.1111/j.1747-0765.2007.00232.x
- Letey, J., Osborne, J, Pelishek, R.E., 1962, Measurement of liquid–solid contact angles in soil and sand, Soil Science, v. 93, p. 149–153.
- Lichner, L., Hallett, P.D., Feeney, D.S., Dugova, O., Sir, M., and Tesar, M., 2007, Field measurement of soil water repellency and its impact on water flow under different vegetation, Biologia, Bratislava, v. 62, no. 5, p. 537–541.
- MacDonald, L.H., and Huffman, E.L., 2004, Post-fire soil water repellency: persistence and soil moisture thresholds, Soil Science Society of America Journal, v. 68, p. 1729–1734, doi:10.2136/sssaj2004.1729
- McGhie, D.A., Posner, A.M., 1981, The effect of plant top material on the water repellence of fired sands and water repellent soils, Australian Journal of Agricultural Research, v. 32, p. 609–620, doi: 10.1071/AR9810609
- METER Group Inc. 2001, USA., WA.
- Neary, D.G., Ryan, K.C., and DeBano, L.F., editors, 2005, Wildland fire in ecosystems: Effects of fire on soil and water, RMRS-GTR-42, v. 4, U.S. Forest Service, Rocky Mountain Research Station, Ogden, UT.
- Olorunfemi, I.E., Ogunrinde, T.A., and Fasinmirin, J.T., 2014, Soil hydrophobicity: an overview, Journal of Scientific Research and Reports, v. 3, no. 8, p.1003-1037, Article no. JSRR.2014.001
- Plaza-Álvarez, P.A., Lucas-Borja, M.E., Sagra, J., Moya, D., Alfaro-Sánchez, R., González-Romero, J., De las Heras, J., 2018, Changes in soil water repellency after prescribed burnings in three different Mediterranean forest ecosystems, Science of the Total Environment, v. 644, p. 247–255.

- Plaza-Álvarez, P.A., Lucas-Borja, M.E., Sagra, J., Zema, D.A., Gonzalez-Romero, J., and Moya D., 2019, Changes in soil hydraulic conductivity after prescribed fires in mediterranean pine forests, *Journal of Environmental Management*, v. 232, p.1021-1027.
- Rau, B.M., Chambers, J.C., Blank, R.R., and Miller, W.W., 2005, Hydrologic response of a central Nevada pinyon- juniper woodland to prescribed fire, *Rangeland Ecology and Management*, v. 58, no. 6, p. 614-622.
- Robichaud, P., 2000, Fire effects on infiltration rates after prescribed fire in Northern Rocky Mountain forests, USA, *Journal of Hydrology*, v. 231–232, p. 220–229, [https://doi.org/10.1016/S0022-1694\(00\)00196-7](https://doi.org/10.1016/S0022-1694(00)00196-7)
- Savadogo, P., Sawadogo, L., Tiveau, D., 2007, Effects of grazing intensity and prescribed fire on soil physical and hydrological properties and pasture yield in the savanna woodlands of Burkina Faso, *Agriculture, Ecosystems, and Environment*, v. 118, p. 80–92.
- Scott, D.F., and Van Wyk, D.B., 1990, The effects of wildfire on soil wettability and hydrological behaviour of an afforested catchment. *Journal of Hydrology*, v. 121, p. 239–256.
- Shakesby, R.A., and Doerr, S.H., 2006, Wildfire as a hydrological and geomorphological agent, *Earth Science Reviews*, v. 74, p. 269-307.
- Shepherd, R.G., 1989, Correlations of permeability and grain Size, *Ground Water*, v. 27, no. 5, p. 633-638.
- Stoof, C.R., Moore, D., Ritsema, C.J., Dekker, L.W., 2011, Natural and fire-induced soil water repellency in a Portuguese shrubland, *Soil Science Society of America*, v. 75, p. 2283–2295.
- Strydom, T., Riddell, E.S., Rowe, T., Govender, N., Lorentz, S.A., le Roux, P.A.L., and Wigley-Coetsee C., 2019, The effect of experimental fires on soil hydrology and nutrients in an African savanna, *Geoderma*, v. 345, p.114–122, <https://doi.org/10.1016/j.geoderma.2019.03.027>
- Varado, N., Braud, I., Ross, P.J., and Haverkamp, R., 2006, Assessment of an efficient numerical solution of the 1D Richards' equation on bare soil, *Journal of Hydrology*, v. 323, p. 244–257.
- Vogel, T. and Cislerova M., 1988, On the reliability of unsaturated hydraulic conductivity calculated from the moisture retention curve, *Transport in Porous Media*, v. 3, p. 1-15.
- Washburn, E.W., 1921, The dynamics of capillary flow, *Physical Review*, v. 17, p. 273–283.

Zhang, R., 1997, Determination of soil sorptivity and hydraulic conductivity from the disk infiltrometer, *Soil Science Society of America Journal*, v. 61, no. 4, p.1024–1030.

Zhang, Y., and Schaap, M.G., 2019, Estimation of saturated hydraulic conductivity with pedotransfer functions: A review, *Journal of Hydrology*, v. 575, p. 1011-1030.

CHAPTER 3: PRESCRIBED FIRE EFFECTS ON SOIL PROPERTIES AND NUTRIENT DYNAMICS IN A FORESTED WATERSHED

3.1. Abstract

Historically, forests in the southeastern USA have been managed with prescribed fire, which has been shown to impact soil moisture dynamics, physical soil properties, and nutrient cycling. The objectives of this study were to evaluate prescribed fire effects on hydrological and physical properties of the soil as well as vertical and lateral movement of key nutrients to further understand immediate short-term (within 2 months post-fire) and chronic long-term (one-year post-fire) temporal changes in soil horizons along a low-relief hillslope where there is a transition from forest to wetland. Using two-way ANOVA and unpaired t-tests, there are no statistical differences in unsaturated hydraulic conductivity or water repellency, within sampling points of the immediate site. Soil properties remained consistent within study sites. There are significant differences found in nutrient concentrations between the immediate and chronic sites for soil A (total P, K, Mn, Fe, Mg, and Al), and soil B (total P, K, Mg, Fe, and Al) horizons. There are also significant temporal changes in nutrients at individual sampling points during the study. Subsurface alterations to total Al and Fe alterations are expressed in the immediate site which could be attributed to the prescribe fire. Alterations to carbon and nitrogen isotopic ratios were significant between sites with evident enrichments found in our immediate site. Spatial alterations could exist along a flat hillslope, due to the nutrient increase found in the soil A horizon near the wetland edge of the immediate site. Overall, a prescribed fire can potentially alter hydrological properties and nutrient dynamics and the effects are integrated into the soil over decadal or even longer temporal scales.

Keywords: Prescribed fire, Hydrological Properties, Loblolly Pine Forests, Nutrient dynamics, Hydraulic Conductivity, Soil Properties, Geographically Isolated Wetlands

3.2. Introduction

In the coastal plain of the southeastern United States, prescribed fire is a common management approach performed with the intention of imitating natural disturbance events, increasing biological diversity, as well as managing both the landscape and commercial timber production (Collins et al. 1998; Mitchell et al. 2002, Boring et al. 2004, Lafon 2010). Specifically, fire-tolerant pine tree species, such as longleaf pine stands, depend on prescribed fires (Fowler and Konopik 2007). Burning the understory helps the trees reach maturity by removing shrubs and competing tree species. In addition, herbaceous plants also benefit from the approach, because they are able to colonize in between fire events which enables them to also successfully reach maturity (Lafon 2010). Prescribed fire has been shown to increase forest productivity by promoting the release of nutrients from plants (Christensen 1977; Lafon 2010). This release of nutrients can potentially affect watersheds as materials are displaced and transported in soil sediments.

Nutrient and sediment export are controlled primarily by waterflow and landscape heterogeneity along a hillslope. Rainfall in particular influences the lateral movement of water along the ground surface and through the subsurface, but flow can vary spatially and temporally (Stieglitz et al. 2003). For example, in certain soil types, where rainfall surpasses evapotranspiration, lateral water movement in the soil profile can be more predominant in the soil (Grayson et al. 1997). Under a dry hydrological state, when there is low hydraulic conductivity horizontally along a hillslope, vertical movement will be prevalent because macropore flow cannot function unless the soil is saturated (Grayson et al. 1997). Hydraulic conductivity has a nonlinear relationship with water content in the soil that can influence macropore flow thereby creating a positive feedback loop where there is an increase in horizontal

subsurface movement under saturated conditions in a catchment along the hillslope (Grayson et al. 1997).

When fire is introduced to the soil, it will volatilize hydrophobic constituents causing compounds to be released to the atmosphere, become translocated, or condensed (Huffman et al. 2001). Once constituents condense after a fire, this can form hydrophobic coating around soil aggregates (Debano and Krames 1966; Savage 1974; Huffman et al. 2001). Because fire introduces changes to organic matter content in the surface soil layer, porosity and pore size decreases (Neary et al. 2005). As porosity and pore size is reduced, soil density increases and there is a loss of macropores, which reduces the capacity for water infiltration (Neary et al. 2005). Specifically, in fire-induced hydrophobic sandy soils, water can flow through preferential flow paths when the pressure head gradient is positive (Rooij 1995). This process is referred to as “fingering” and the preferential flow paths are referenced as “fingers,” which influences the leaching of substances (Rooij 1995). In the top hydrophobic soil surface, water flows laterally towards the preferential flow paths and then moves vertically until it reaches the B or C horizon. Capillary forces cause water to then disperse (Rooij 1995). Research has shown that prescribed fires can have variable effects on the strength of hydrophobicity and infiltration rate (Debano and Krames 1966; Huffman et al. 2001; Savadogo et al. 2007; Stoof et al. 2011; Strydom et al. 2019).

As fire removes vegetation, this can also expose the soil surface to the effects of rainfall causing crusting (Moyo et al. 1998; Mills and Fey 2004; Savadogo et al. 2007). As rain infiltrates the soil, clay particles are dispersed thus reducing infiltration (Hillel 2004; Savadogo et al. 2007). Clay dispersion can result in the reduction of macroporosity, water percolation, aeration, and an increase in clogage (Brady and Weil 2008). In sandy soils, clay and silt movement is slow as particles translocate from the A to a B horizon, and changes may not be

visible within shorter time spans of 1-2 years (Birkeland 1999). If clay is moving through water suspension, clay content will be high in the B horizons and low in the A and C horizons. Clay cannot disperse if the soil has high electrolytes and if colloids have a positive charge (Birkeland 1999). Like clay, silt can be suspended in water as long as pore spaces permits in the soil (Birkeland 1999). Soil texture--consisting of the relative percent of sand, clay, and silt-- affects the depth of leaching in soils where it will be greater in coarser particles and less in fine-grained material (Birkeland 1999).

Studies have found potential prescribed fire effects to soil structure (Chief et al. 2012), hydrological properties (Gonzalez-Pelayo et al. 2010, Robichaud et al. 2008; Badia-villas et al. 2020; Sharenbroch et al. 2012; Savadogo et al. 2007; Strydom et al. 2019; Stoof et al. 2011), and nutrient dynamics (Coates et al. 2018; Lavoie et al. 2010) separately. Prescribed fire effects to longleaf pine forest soils have been documented in the Southeast (Richter et al. 1982; McKee 1982; Boring et al. 2004; Boyer and Miller 1994; Lavoie et al. 2010; Butnor et al. 2020), but few have focused on soils within forested geographically isolated wetland (GIW) watersheds (Battle and Golladay 2003; Jansen et al. 2019). Using a muffler furnace to simulate prescribed fire events, Battle and Golladay (2003) found an increase in bioavailable phosphorous, pH, dissolved organic carbon, alkalinity, and ammonium to water samples exposed to the burned soils. Jansen et al. (2019) found significant decreases in total P concentrations in wetlands that were grazed and treated with prescribed fire. The mentioned studies have all highlighted impacts to soil properties, hydrological properties, and nutrient cycling separately but nevertheless there exists a knowledge gap addressing the combined prescribed fire effects to soil properties, hydrological properties, and nutrient dynamics along a gradient in forested geographically isolated wetland watersheds in particular.

In this study, I investigated the immediate short-term (over 2 months) effects a recent prescribed fire treatment has on soil nutrient, hydrological, and texture dynamics and compared them to chronic prescribed fire effects one-year post-fire. The research objectives are: (1) document alterations to soil moisture dynamics immediately after a prescribed fire, indicated by changes to hydrophobicity and unsaturated hydraulic conductivity in the surface horizon (2) determine if prescribed fire can increase the movement of nutrients with depth in a soil profile on a short temporal scale and (3) identify the immediate and chronic effects prescribed fire has on nutrient content as well as carbon and nitrogen isotopic ratios in the surface soil horizon when compared to the subsurface. I hypothesize that prescribed fire will cause nutrient losses in the surface horizon on short temporal scales, due to mineralization and eluviation of materials, as compared to the subsurface. Furthermore, I expect alterations to carbon and nitrogen isotopic ratios along the slope immediately after the fire. In comparison, the chronic effects to the landscape should diffuse given the year since the last fire. I also hypothesize that there will be short-term changes to hydrological properties by the recent fire. Overall, I am interested in predominant short-term changes to soil dynamics and how it can affect nutrient cycling in a GIW watershed while determining if chronic long-term effects will still be expressed after one year since a prescribed fire.

3.3. Methods

The study area is a managed long leaf pine forest with GIWs at the Jones Center at Ichauway, a 117.36 square kilometer research site located in the Dougherty Plain of Georgia within the Coastal Plain physiographic province (Figure 1). The study site has a karst topography with dynamic interaction between groundwater and surface water. Two wet-mesic longleaf pine savanna forested sites were selected to represent immediate and chronic effects respectively—

site W37, which was burned during the study period, and site W29, which was burned the previous year (Figure 1). In the immediate site (W37), soil samples were collected along one transect that was established vertically along a low relief hillslope running from an upland forested site towards the wetland extending 25 meters from a midpoint of 70 meters where an additional transect was placed horizontally (Figure 2). Similarly, in the chronic site, a transect was established vertically running 25 meters from a midpoint of 42.5 meters with the other transect intersecting horizontally at this point. Soil cores were taken at four end points of each transect at both sites. Sampling points are referred to by their location -- upland, transition zone 1 and transition zone 2 across the mid-point, and wetland edge near the land depression (Figure 2). For the purpose of this study, field work and sampling occurred over three months within a single calendar year (2021), before a prescribed fire (T1), after the fire, and after a large rain event (T2).

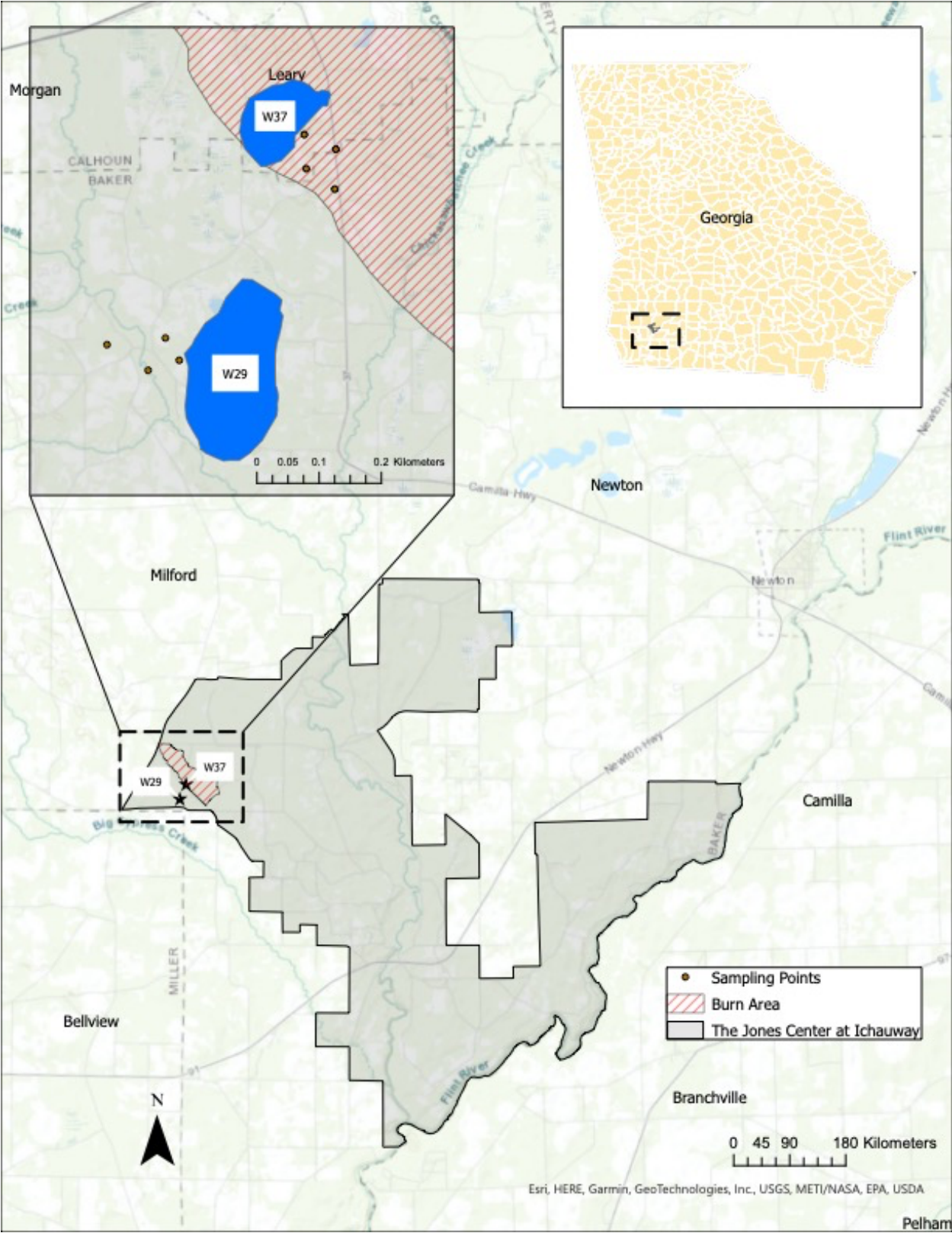


Figure 1. Map illustrating our study area at the Jones Center at Ichauway in Georgia, USA

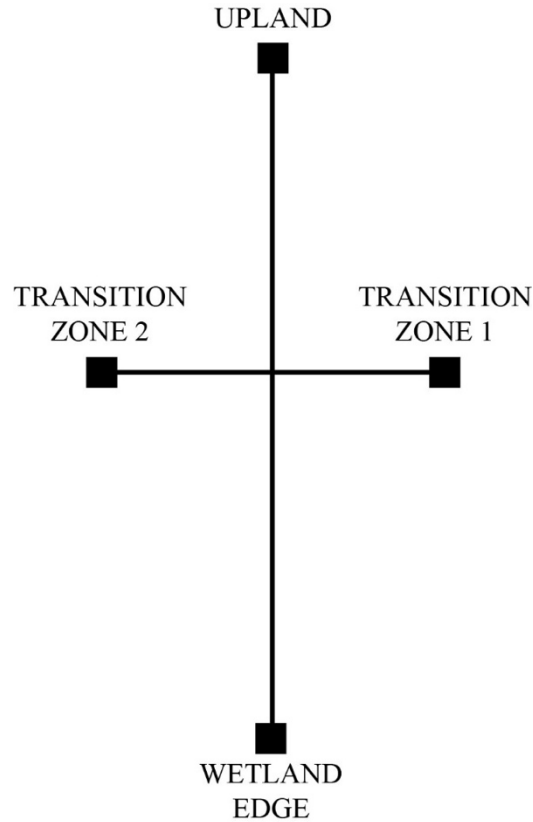


Figure 2. Field setup schematic for immediate site and chronic site with established transect and 4 soil sampling points along a low-profile hillslope.

According to the Web Soil Survey, both study sites have soils belonging to the Tifton loamy sand and Grady fine sandy loam map units with drainage class being well-drained to poorly drained. Sites are relatively flat with a topographic relief range of 100-450 feet above mean sea level (Soil Survey Staff, accessed 2022). The chronic site (W29) watershed is approximately 0.14 square kilometers surrounding a 0.025 square kilometer wetland, while the immediate site (W37) is approximately 0.053 square kilometers surrounding a 0.0089 square kilometer wetland. Both watersheds have been managed with prescribed fire treatments approximately every two years from 2018-2021. The chronic site contains a cultivated area which was not present in our immediate site. Water levels in our immediate site initially decreased overtime and began increasing after a large rainfall event (Figure 3). Although there is

limited data available for the water levels in our chronic site, we expect a similar pattern due to the close proximity between watersheds.

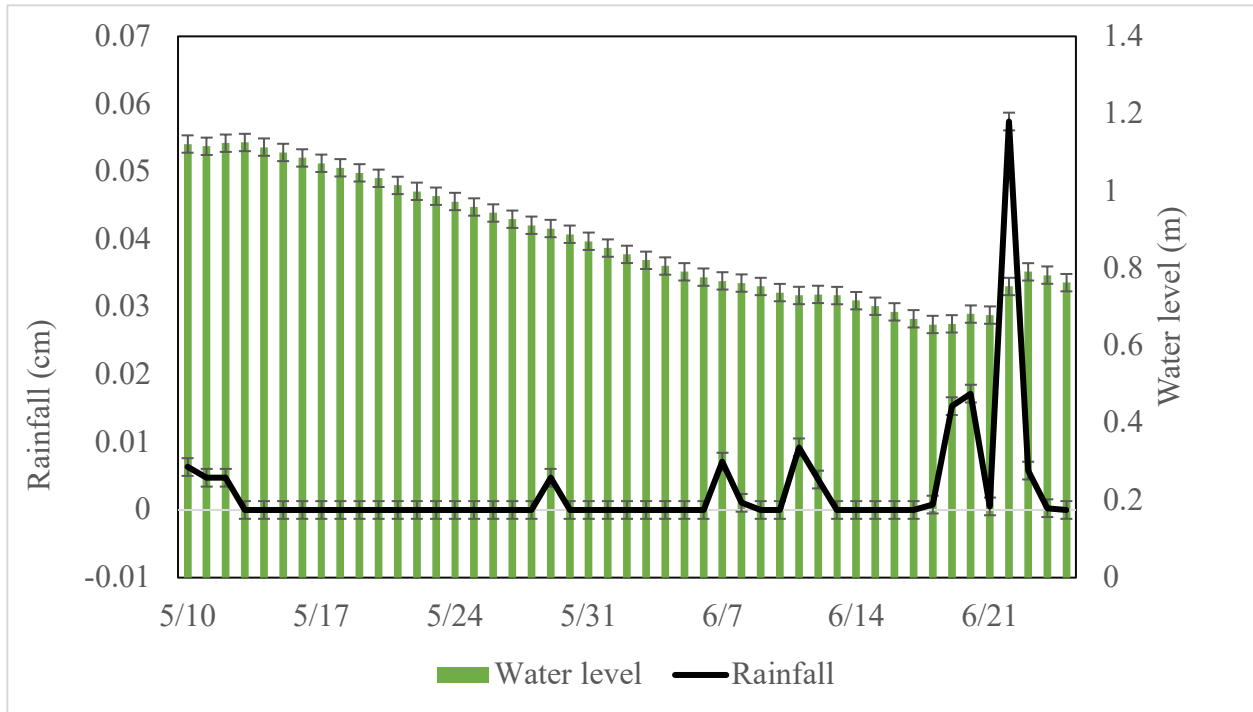


Figure 3. Wetland water levels and rainfall amounts measured in the immediate study site (provided by Dr. Steven Brantley at the Jones Center at Ichauway).

3.3.1. Soil Infiltration Sampling

We measured soil infiltration rates at all four points in the immediate site using a minidisk infiltrometer, with a suction rate of 2 cm and radius rate of 2.25 cm, pre-fire (T1) and post-rainfall (T2). We took measurements within a day after the fire at the upland area and transition zone 1. Water and ethanol infiltration rate was determined by performing calculations using the formula (METER 2021):

$$I = S_w \sqrt{t} \quad \text{(Equation 1)}$$

where I (cm) is the cumulative infiltration, S_w ($\text{cm} \times \text{s}^{-1}$) is water sorptivity, and t (s) is the square root of time in seconds (METER 2021). Unsaturated hydraulic conductivity (K) ($\text{cm} \times \text{s}^{-1}$) was then determined by using the equation:

$$K = C_I/A \quad (\text{Equation 2})$$

where C_I ($\text{cm} \times \text{s}^{-1}$) is the slope of the cumulative infiltration rate per square unit of time and A was determined to be 2.4286 following van Genuchten variable parameters used for the loamy sand soil type in this region (METER 2021). Ethanol sorptivity was measured by using the formula:

$$I = S_e \sqrt{t} \quad (\text{Equation 3})$$

where I (cm) is the cumulative infiltration, S_e ($\text{cm} \times \text{s}^{-1}$) is ethanol sorptivity, and t (s) is the square root of time in seconds. Water repellency (R), or also referred to as hydrophobicity, could be determined with the use of the equation:

$$R = 1.95 ((S_{ethanol})/(S_{water})) \quad (\text{Equation 4})$$

where the slope of the line for ethanol sorptivity ($S_{ethanol}$) ($\text{cm} \times \text{s}^{-1}$) and water sorptivity (S_{water}) ($\text{cm} \times \text{s}^{-1}$) is utilized to perform such calculation (Hallett et al. 2001). We collected separate surface soil samples for bulk density in the laboratory.

3.3.2. Soil Laboratory Analysis

We collected 16 soil core samples with a hand auger, split in between 2 separate sampling periods with 8 retrieved pre-fire (T1) and the other 8 post-fire after the prescribed fire and a rain event (T2) at each study site. Grain size was determined by using both a sieving method to remove coarse particles and the micropipette method to analyze fine particles (Miller

and Miller 1987). Bulk density was evaluated by weighing each soil sample separately and then determining the volume of the material where we report it as g/cm^3 (Brady and Weil 2008). The loss on ignition methodology test was used to estimate the percent of organic matter present and organic C, as determined using the conversion factor of 0.469 (Heathcote and Downing 2012), within collected soil samples where samples are first oven dried and then placed in a muffler furnace at a temperature of 500°C for 3 hours (Storer 1984).

Surface and subsurface samples from the soil cores were analyzed for grain size, bulk density characteristics, organic matter, and nutrient concentrations. Samples were sent to Waters Agricultural Laboratories, Inc. located in Camilla, Georgia for elemental analysis, with the use of an Inductively Coupled Plasma Mass Spectrometry (ICP-MS) following nitric acid digestion in a heated block, to evaluate the total carbon (C), phosphorus (P), potassium (K), manganese (Mn), iron (Fe), calcium (Ca), magnesium (Mg), and aluminum (Al) present in our samples (EPA 6010B). Samples for carbon and nitrogen isotopic ratios were sent to the University of Arkansas Stable Isotope lab in Fayetteville, Arkansas. For organic carbon, samples were treated with HCL for approximately 2 hours to remove carbonates prior to analysis (E. Pollock, Personal Communication, 2022).

3.3.3. Statistical Analysis

A principal component analysis was performed to evaluate ordination of nutrients in our immediate site under pre-fire and post-fire conditions (SAS Institute Inc. 2008). Two-way ANOVA analyses were used to evaluate changes to soil properties, in terms of bulk density and soil texture, alterations to nutrient pools, and effects to hydrological properties, referred to as unsaturated hydraulic conductivity and water repellency. Changes in hydraulic conductivity and water repellency, with the use of logarithmic values, within the soil A horizon were evaluated

under the pre-fire, immediately post-fire, and post-fire with large rain event condition using unpaired t-tests. Unpaired t-tests were utilized to evaluate if the differences between pre- and post-fire values at the same sampling point locations were significantly different between the immediate and chronic site in terms of alterations to soil texture, nutrients, or carbon and nitrogen isotopic signatures.

3.4. Results

Although the study sites are in close proximity to each other and have similar soil texture, results show heterogeneity in soil nutrients between the immediate and chronic watershed. I also observe temporal changes to hydrological properties at the immediate site before and after a large rain event. Temporal changes in nutrient content in surface and subsurface horizons (referred to as A and B horizons respectively moving forward) are evident. There appears to be some nutrient movement in surface A horizons along the hillslope. Evident alterations to carbon and nitrogen isotopic ratios also occur in the A and B horizons between watersheds.

3.4.1. Soil Bulk Density and Texture

Bulk density is not significantly different between sampling times or among our immediate and chronic sites, as determined by two-way ANOVA, with $p\text{-value} > 0.05$. Differences within each sampling location are also not significant, as indicated by unpaired t-tests (Table A18-A19). In the soil A horizon, grain size analysis shows soil texture, loamy sand, is homogenous at all sampling points in both the immediate and chronic sites with no significant temporal changes, as determined by unpaired t-tests (Table A22-A23). The relative percent of sand and clay is significantly different between sites, as determined by two-way ANOVA with $p\text{-value} < 0.05$. Similarly, in both immediate and chronic sites, soil texture in the B horizon is consistent, identified as sandy clay loam, loamy sand, or sandy loam, with no statistical

differences (Table A24-A25). Overall, soil textures in both watersheds are in accordance with the web soil survey for the A and B horizons (Web soil Survey accessed 2022). A complete data set with statistical calculations is available in Appendix A.

Statistical analysis shows soil texture within the A horizon is consistent within each watershed, but there is variability between the two sites. Sand content ranges between 77.5% and 83.7% in the immediate site and 78.4% and 81.1% in the chronic site. Relative silt content increases and clay content decreases from T1 to T2 at both transition zone sampling points. At the wetland edge, relative sand content decreased from T1 to T2 by about 5%, while silt and clay content increased by 4.5% and 0.5% respectively. In the chronic site, fluctuations at all points were minor with no obvious pattern.

At the immediate site, sand content varies greatly from 49.5% to 84.4% and 57.4% to 72.7% at the chronic site in the B horizon. Fluctuation in silt and clay content was not uniform within or between the watersheds. Of note, relative sand content increased by about 23.3% and clay content decreases by 25.3% at the upland sampling point (approximately 37 cm in depth). This change is not evident in other grain size samples in this auger core or at other sampling points, suggesting it is an outlier.

3.4.2. Unsaturated Hydraulic Conductivity and Water Repellency

Overall, there is variability in unsaturated hydraulic conductivity and water repellency within the immediate site. As predicted, water repellency increased immediately after the fire at the Transition Zone 1 sampling point and after the rain event (Table 1). At the upland and both transition zone sampling points, water infiltration decreased immediately after the fire and increased post-rainfall. The post-rainfall measurements indicate the soil was saturated. Overall, there is variability in unsaturated hydraulic conductivity and water repellency within the

immediate site. Although there were evident variabilities in unsaturated hydraulic conductivity and water repellency within sampling points, they were not statistically significant according to unpaired t-tests, with $p\text{-value} > 0.05$ within the sampling points in both sites (Table B9-B10).

Table 1. Calculated water repellency and unsaturated hydraulic conductivity for all sampling points in immediate site.

	Water Sorptivity (S_w) (cm x s^{-1})	Ethanol Sorptivity (S_e) (cm x s^{-1})	Water Repellency (R) (cm x s^{-1})	Unsaturated Hydraulic Conductivity (K) (cm x s^{-1})
Pre-Fire (T1)				
Upland	0.0018	0.0053	5.74	7.55×10^{-4}
Transition Zone 1	0.0020	0.0063	6.14	8.18×10^{-4}
Transition Zone 2	0.0020	0.0043	4.19	8.41×10^{-4}
Wetland Edge	0.0020	0.0008	0.78	8.41×10^{-4}
Post-Fire				
Upland	0.0011	0.0024	4.25	4.36×10^{-4}
Transition Zone 1	0.0003	0.0048	31.2	1.32×10^{-4}
Post-Rainfall (T2)				
Upland	1	1	1.95	2.80×10^{-2}
Transition Zone 1	0.0018	1	1083.33	7.31×10^{-4}
Transition Zone 2	0.0341	1	57.18	1.40×10^{-2}
Wetland Edge	-0.0550	0.0800	-2.84	-2.26×10^{-2}

3.4.3. Nutrient Content

Nutrient analysis of the soil cores taken at both watersheds show differences within sites and between sites (Table 2). Total P, K, Mn, Mg, and Fe contents are significantly different between sites in A horizon samples while total P, K, Mg, Fe, and Al changes are significant in the B horizon samples (Table C1-C4). There are significant changes in total C, Mn, and Al between study sites for the surface soil A horizon and Mn in the subsurface soil B horizon. Total C increases in the A horizon from T1 and T2 at all sampling points except the wetland edge in

the chronic site. However, in the B horizon, concentrations vary slightly within and between sites over the period of the study trending towards a slight decrease. Mn levels in the soil remain constant from T1 and T2 except for an increase from no measurable concentration to 0.26 mg/g and 0.05 mg/g in the A and B horizons respectively after the rain event at the wetland edge sampling point in the immediate site. Mn concentrations within the B horizon between the chronic and immediate sites are significantly different as indicated by unpaired t-tests with a p-value < 0.05. Total Al concentrations in the soil A horizon fluctuate at all sampling points, generally increasing from T1 to T2 in the immediate site, while generally decreasing in the chronic site. This pattern is the same for the B horizon at the immediate site, but there is negligible Al concentration in the B horizon at the chronic site. There are small fluctuations in Fe, Ca, and Mg concentrations between sampling times at both sites, but there is no discernable pattern and P, K, and Na are very low with no significant change at all sampling points and times. Nutrient concentrations overall are significantly different between the immediate and chronic site; therefore, it is difficult to attribute induced alterations to the legacy effect of the prescribed fire itself, precipitation, or other unexplored factors.

Principal component analysis was performed to differentiate between pre-fire (T1) and post-fire/rain (T2) conditions for soil A and B horizons together at the immediate site (Figure 4). Principal components 1 and 2 explained 42.8% and 22.8% of the variability in the data respectively, that in pre-fire condition, P, Ca, and organic C were positively correlated, as determined by eigenvector values, and ordinated together while the elements K and Mg were positioned towards the post-fire condition (see Appendix C).

Table 2. Nutrient concentrations in immediate and chronic sites under Time 1 (T1) and Time 2 (T2).

		C (%)	P (mg/g)	K (mg/g)	Mn (mg/g)	Fe (mg/g)	Ca (mg/g)	Mg (mg/g)	Na (mg/g)	Al (mg/g)
Immediate Site T1	Upland									
	A Horizon	1.54	0.03	0.01	0.08	2.53	0.59	0.10	0.01	3.42
	B Horizon	0.95	0.04	0.02	0.02	-	0.46	0.16	-	-
	Transition Zone 1									
	A Horizon	1.59	0.04	0.02	0.12	3.19	0.49	0.13	0.05	3.68
	B Horizon	0.78	0.05	0.05	0.02	-	0.46	0.19	0.05	11.45
	Transition Zone 2									
	A Horizon	1.42	0.03	0.02	0.13	2.38	0.60	0.16	0.05	4.71
	B Horizon	0.58	0.02	0.02	0.05	4.20	0.36	0.15	0.05	7.31
	Wetland Edge									
A Horizon	1.39	0.03	0.01	0.00	4.28	0.34	0.08	0.05	4.16	
B Horizon	0.83	0.02	0.01	0.00	2.82	0.29	0.10	0.05	5.98	
Chronic Site T1	Upland									
	A Horizon	1.55	0.07	0.04	0.29	5.26	0.42	0.18	0.06	8.02
	B Horizon	0.91	0.05	0.05	0.15	-	0.37	0.20	0.05	-
	Transition Zone 1									
	A Horizon	1.15	0.05	0.05	0.41	3.27	0.49	0.18	0.04	6.07
	B Horizon	0.63	0.05	0.06	0.16	-	0.37	0.22	0.04	-
	Transition Zone 2									
	A Horizon	1.90	0.07	0.03	0.23	4.82	0.81	0.23	0.04	7.16
	B Horizon	1.01	0.09	0.08	0.05	-	0.55	0.29	0.06	-
	Wetland Edge									
A Horizon	1.80	0.06	0.03	0.31	5.08	0.85	0.20	0.06	6.89	
B Horizon	0.69	0.06	0.05	0.02	-	0.46	0.22	0.05	-	
Immediate Site T2	Upland									
	A Horizon	1.62	0.03	0.02	0.08	2.64	0.87	0.14	0.04	4.27
	B Horizon	0.85	0.04	0.04	0.02	-	0.60	0.19	0.05	-
	Transition Zone 1									
	A Horizon	1.97	0.04	0.02	0.11	3.45	0.49	0.14	0.05	4.01
	B Horizon	0.73	0.03	0.03	0.03	-	0.42	0.17	0.05	9.08
	Transition Zone 2									
	A Horizon	1.75	0.03	0.02	0.14	2.17	0.55	0.15	0.04	4.47
	B Horizon	0.65	0.02	0.02	0.07	4.09	0.41	0.18	0.06	8.46
	Wetland Edge									
A Horizon	2.30	0.06	0.03	0.26	2.75	0.99	0.23	0.04	4.29	
B Horizon	0.68	0.02	0.02	0.05	5.59	0.44	0.18	0.05	7.14	
Chronic Site T2	Upland									
	A Horizon	2.18	0.06	0.05	0.31	4.44	0.64	0.20	0.05	7.27
	B Horizon	0.81	0.09	0.09	0.03	0.00	0.48	0.32	0.06	-
	Transition Zone 1									
	A Horizon	1.72	0.06	0.04	0.42	3.25	0.65	0.19	0.05	5.38
	B Horizon	0.79	0.05	0.06	0.11	-	0.43	0.25	0.05	-
	Transition Zone 2									
	A Horizon	2.18	0.09	0.04	0.24	4.85	1.01	0.32	0.04	7.38
	B Horizon	0.84	0.09	0.08	0.04	-	0.45	0.31	0.06	-
	Wetland Edge									
A Horizon	1.67	0.04	0.01	0.25	3.25	0.55	0.14	0.06	5.49	
B Horizon	0.64	0.05	0.04	0.02	-	0.51	0.20	0.07	-	

*- indicate concentrations <0.000015 mg/g

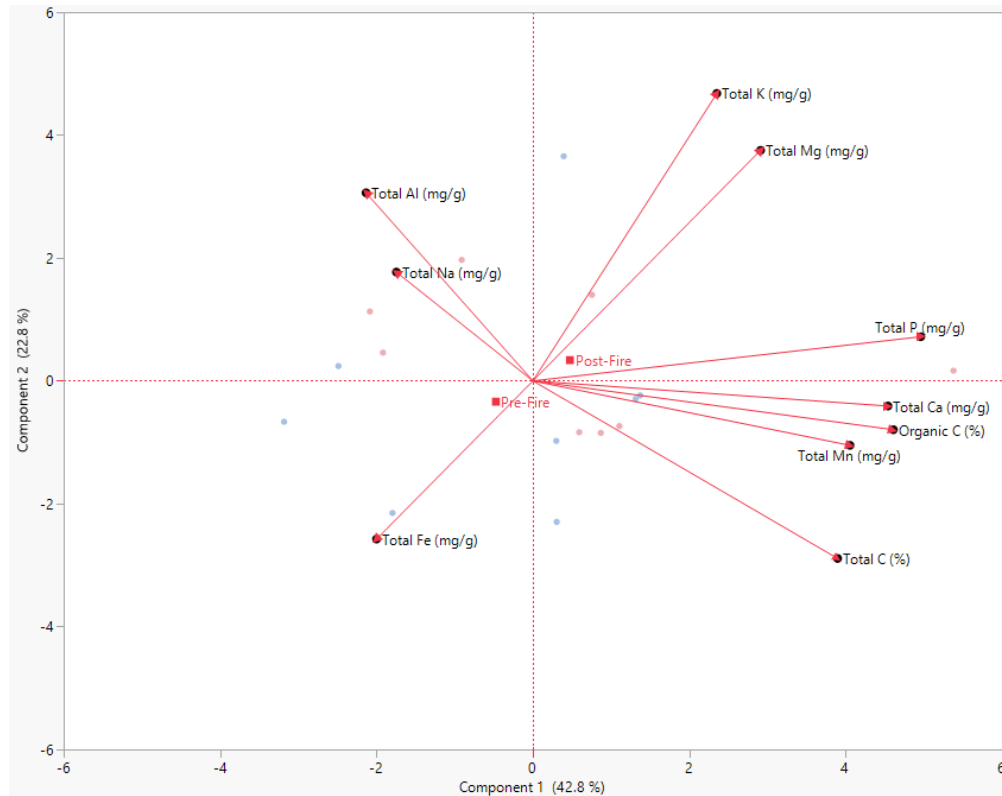


Figure 4. Principal component analysis biplot portraying nutrient pools across immediate site under pre-fire (blue) and post-fire (red) conditions in A and B horizons.

3.4.4. Carbon and Nitrogen Isotopic Ratios

Carbon and Nitrogen isotopic ratios are statistically different between the immediate and chronic sites, as indicated by the two-way ANOVA results with p -value < 0.05 . There are small observable temporal changes within each watershed between T1 and T2 (Table D2-D5). In the A horizon of the immediate site, carbon isotopic ratios, or $\delta^{13}\text{C}$, decrease in the upland area from -26.39‰ to -26.54‰ and in wetland edge from -26.30‰ to -26.78‰ (Figure 5a). In transition zone 1, $\delta^{13}\text{C}$ ratio increases from -25.76‰ to -25.06‰ . Similarly in transition zone 2, carbon isotopic ratio increases from -26.80‰ to -26.00‰ . Changes to carbon isotopic ratios are minimal in the B horizon within samples collected (Figure 5b). Despite there being slight changes to carbon isotopic ratios in our immediate site, there is evident carbon depletion in both upland and wetland edge localities. There was also enrichment in the transition zones. In the chronic site,

changes to carbon isotopic ratios are minimal in the upland area, where there is a partial decrease from -25.32‰ to -26.28‰ (Figure 5c). In the wetland edge, $\delta^{13}\text{C}$ ratio increases from -24.28‰ to -24.17‰, and there was also an increase in transition zone 1 from -24.07‰ to -23.98‰ while there was a decrease in transition zone 2 from -25.07‰ to -25.17‰. Comparably to our immediate site, there are minimal changes present in the soil B horizon (Figure 5d). Our chronic site shows minimal carbon enrichment in upland and wetland edge area, but depletion to transition zones, which completely differed from our immediate site. Unpaired t-tests, with p-value > 0.05, showed that changes in both horizons are not significant among the sampling points nor between sites (Table D2-D5).

Despite there not being statistical significance pertaining to each paired sampling point, as determined by unpaired t-test, with p-value > 0.05, observable changes to nitrogen isotopic ratios, or $\delta^{15}\text{N}$, are minimal in the B horizon but are more prevalent in the A horizon. In the immediate site, there is an increase in the upland area from 1.26‰ to 4.08‰, partial increase in transition zone 1 from 2.61‰ to 2.65‰, and an increase in transition zone 2 from 2.57‰ to 5.05‰. In the wetland edge, $\delta^{15}\text{N}$ decreases from 1.99‰ to -1.22‰ (Figure 5a, b). In the chronic site, there is an overall decrease in upland area, from 3.85‰ to 3.42‰, and in transition zone 1 from 4.30‰ to -3.40‰ (Figure 5c, d). Nitrogen isotopic ratio increases in transition zone 2 from 2.57‰ to 5.05‰ and decreases in wetland edge from 1.99‰ to -1.22‰. Overall, there are slight visible changes in carbon and nitrogen isotopic signatures along the sampling points of the study sites (see Appendix D).

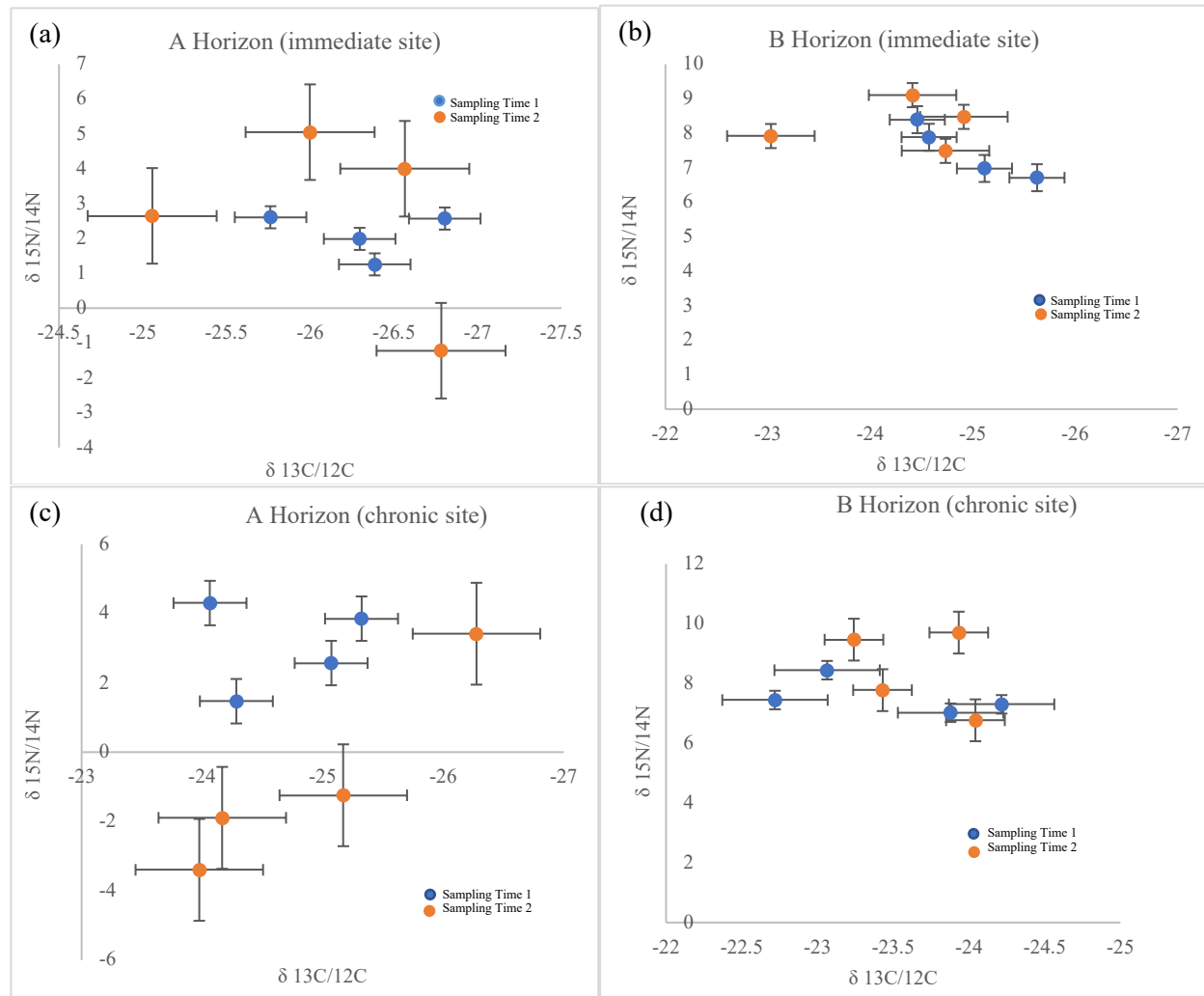


Figure 5. Carbon and nitrogen isotopic ratios for soil A (a,c) and B horizons (b,d) in immediate and chronic site under sampling time 1 (blue) and sampling time 2 (orange) conditions where $n=8$ in A horizon and $n=8$ in B horizon.

3.5. Discussion

3.5.1. Soil Properties

Supporting our hypothesis that prescribed fire should not significantly alter soil, temporal changes to bulk density or soil texture are not significant between study sites, following previous research (Kennard and Gholz 2001, Sharenbroch et al. 2012). Since both immediate and chronic sites have been managed with fire between 2018-2021, and show uniformity in soil texture and

bulk density, prescribed fire is not a primary control on these properties within our study area. As compared to wildfire, carefully managed prescribed burns are designed to clear the understory, but not burn hot enough to damage mature healthy trees therefore should not negatively impact soil. In terms of soil texture, clay is the most sensitive to fire intensity. Clay particles start to break down at 400°C and will be destroyed at temperatures > 700°C (Verma and Jayakumar 2012). Therefore, prescribed fire effects may be more significant in soils with higher clay content but have minimal effect on the sandy soils found in our study site.

3.5.2. Hydrological Properties

Rejecting the hypothesis regarding short-term changes to hydrological properties within our immediate site, in terms of unsaturated hydraulic conductivity and hydrophobicity, there are no statistical differences in unsaturated hydraulic conductivity and water repellency measurements found in the immediate site. Despite this, there is evidence of temporal small-scale alterations to hydrological properties within sampling points at the immediate site that suggests that within the first few days after a prescribed fire, water repellency increases. In the Transition Zone 1 sampling point, water infiltration decreases immediately after the fire while ethanol infiltration increases indicating water repellency and research has discussed that unsaturated hydraulic conductivity can be affected by water repellency (Lichner et al. 2007). Water repellency also increases after a large rain event which could be an error when gathering the data because water repellency should disappear within the soil once soil moisture surpasses 12-25% (Huffman et al. 2001). The short-term changes to water infiltration in this study are similar to what was observed in Mediterranean pine forests and shrublands (Gonzalez-Pelayo et al. 2010; Robichaud et al. 2008; Badia-villas et al. 2020). Similar to Sharenbroch et al. (2012), changes to hydrophobicity were not significant. It is important to note that water repellency was

relatively high at T1, prior to the fire, therefore it naturally existed in our soil samples at the immediate site (e.g. Huffman et al. 2001). Overall, ethanol infiltration increased while water infiltration decreases immediately post-fire, this combined with the increase in unsaturated hydraulic conductivity after the large rain event, illustrates that water infiltration capacity can change on very short temporal scales.

Once water infiltration decreases and water repellency increases in the sandy soil, this may promote the accumulation of nutrients in the surface horizon or could lead to the leaching of nutrients through preferential flowpaths (e.g. fingering). Rainfall intensity can have an effect as the soil becomes saturated and more pore spaces are filled. As saturation increases, this could have potentially facilitated lateral nutrient movement in the soil leading to surface runoff which could affect accumulation in the wetland itself that may impact water quality. Despite studies showing fire significantly affecting soil water repellency and hydraulic conductivity (Savadogo et al. 2007; Strydom et al. 2019; Stoof et al. 2011), we were unable to tease out this relationship with our sampling. In the future, more measurements could be taken across a hillslope, such as installing in situ soil moisture data loggers, to determine overall effects prescribed fires have on hydrological properties.

3.5.3. Nutrient Concentrations

There is significant variability between the immediate and chronic sites with respect to total nutrient concentrations within and between the two watersheds, but no strong evidence of nutrient losses in the A horizon. The data collected for this study cannot resolve if the effects to nutrient content, in the surface and subsurface horizons, are due to repetitive use of prescribed fire or influenced by other factors such as rainfall intensity. The variability in Mn and Fe concentrations in A horizon samples and P, K, and Fe concentrations in B horizon samples is

similar to what was found in previous coastal plain research focused on short- and long-term effects of prescribed fire (Coates et al. 2018). Significant changes and increases to K and Mg concentrations found in our A horizon is similar to what other researchers found in the top 5-10 cm of soil, 1-3 years after a prescribed fire (Lavoie et al. 2010). In our study, there is a positive correlation between Mg and K concentrations, which, following previous research, can be attributed to an increase in concentrations of both elements after a burn due to the deposition of wood ash. Research has also shown that prescribed fire can increase extractable concentrations of Mg, K, and Ca concentrations which can increase soil pH and affect nutrient availability (Park et al. 2005; Pereira et al. 2011). In our study, total Al and Fe are the only elements that are of low concentration, notably in the B horizon samples from the chronic site. It is difficult to conclude if such changes are due to the prescribed fire or other factors, such as the agricultural plots in the chronic site. The significant changes in P in the surface and Mg as well as Al concentrations in the subsurface have implications that bear further investigations.

In both watersheds, there are significant changes in total C, Mn, and Al concentrations within A horizon points and Mn concentrations in the B horizon. Our chronic site exhibited higher nutrient levels, in surface horizons, than in our immediate site, but the mean of the changes in total C concentration within sampling points of the immediate site is higher than the differences present within the chronic site which indicates prescribed fire has an immediate effect. The increase of C concentrations is expected as biomass is burned. For example, Butnor et al. (2020) documented a short-term pulse of C in the topsoil after a fire. The increases in total Mn within the immediate and chronic sites can also be attributed to the fire, since Mn is released by the burning of pine trees after a fire (Gonzalez-Parra et al. 1996; DeMarco et al. 2005).

In the wetland edge sampling point in the immediate site, there are increases in total C, P, Mg, K, Ca, and Mn concentrations which I interpret as a short-term response to fire. Because the wetland edge is anoxic and there is low microbial activity, the observed accumulation of nutrients in the soil could be due to the increase in nutrient stocks and nutrient losses from upslope immediately after the fire and rain event. The heterogeneity in infiltration rates and soil properties across the slope gradient from upland to the wetland edge could potentially affect nutrient export and movement. More research is needed to determine if there is a change in total C, P, Mg, K, Ca, and Mn concentrations immediately after a fire along the slope before and after a rain event. In order to understand how prescribed fires impact nutrient dynamics in forested watersheds, future studies should investigate how changes to hydrological and soil properties affect nutrient transport across a slope gradient.

Future studies could fractionize the total nutrient concentrations to determine what forms are available for uptake. Although we focus on changes to total nutrient stocks in soil A and B horizons, research has shown that prescribed fires can increase extractable concentration forms of P, Mg, K, and Ca in the top surface horizon (Kennard and Gholz 2001). Changes in concentrations has been ascribed to the potential dispersion of cations from organic matter resulting from the burn. Overall, we found significant changes to total nutrient concentrations both immediately post-fire as well as chronic effects one year after a prescribed fire. Burning approximately every two years, as documented in our chronic site, could have potentially contributed to the high nutrient levels present in the watershed because of the ash and partial burning of organic matter (Rau et al. 2009; Alcaniz et al. 2016; Alcaniz et al. 2018). Based on the higher nutrient levels in the chronic site, the effects of fire can be seen over a year after a fire, rejecting our hypothesis that effects would have dissipated after one year. Although we do not

know the nutrient concentrations at the time the chronic site was burned, other research has shown significant long-term prescribed fire effects to P (McKee 1982), Mg (Wells 1971) Al, Mn, and Fe (Coates et al. 2018) concentrations.

3.5.4. Carbon and Nitrogen Isotopic Ratios Alterations

Rejecting our hypothesis about immediate changes in isotopic ratios, the alterations to carbon and nitrogen isotopic signatures are not statistically significant. In our managed longleaf pine forested sites, our overall carbon isotopic ratios in the A horizons of both our immediate and chronic watersheds show that the dominant groundcover understory species followed a C₃ photosynthetic pathway, comprising of composites, grasses, legumes, and shrubs, all of which are commonly found in burned pine stands (Kirkman and Jack 2017; Baniya et al. 2022).

Even though our sites reside in a longleaf pine-wire grass ecosystem, our carbon isotopic ratios did not show a dominance of C₄ species as was found in a fire managed long-leaf pine-wiregrass savanna (Schafer et al. 2013). Despite wire grass species having a C₄ photosynthetic pathway, our results show that carbon inputs from this species are not as dominant in the surface A horizon as that of C₃ species. Carbon inputs from C₃ species to soil organic matter, can alter carbon isotopic signature if there is a higher percent coverage of this type than of C₄ species in the region (Schafer et al. 2013). The region around the Jones Center was dominated by wire grass species until the late 1800s. The wire grass land cover was displaced by logging and row crop cultivation of corn, cotton, and peanuts from the 1900s to today (Holland et al. 2019). Currently, the Jones Center consists of second growth long-leaf pine forests (Holland et al. 2019). Because this area is managed with prescribed fire, C₃ species were not competitively excluded by wire grass allowing the species to coexist (Kirkman et al. 2001).

As previously discussed, total C concentrations are significant and the mean of the differences in sampling points within the immediate site is greater than that of the chronic site where we see increases post-fire which could have altered carbon isotopic ratios. In our immediate site, changes were minimal, except carbon isotopic ratios increases in both transition zone A horizon samples. This could be due to the burning of biomass, or the type of burned foliage species. The B horizon is more enriched in $\delta^{13}\text{C}$ than the A horizon which is typical of soils with C_3 vegetation (Balesdent et al. 1993). As organic matter decays, it travels downward in the soil profile where it is stored representative of old buried carbon stocks. One study found that $\delta^{13}\text{C}$ enrichment with depth is not as prevalent in pine forests when compared to deciduous forests, but this is typical of established pine stands with ages of less than 100 years (Balesdent et al. 1993; Baniya et al. 2022). The overall enrichment of $\delta^{13}\text{C}$ seen in our immediate site is similar to what researchers found immediately after a prescribed fire and ascribed the change to ash input or precipitation (Tahmasbian et al. 2019). Ale et al. (2018) found that leaf $\delta^{13}\text{C}$ decreased with increasing rainfall which could explain our $\delta^{13}\text{C}$ signatures. Because our study sites consisted of high percentages of sand content it is also important to consider soil texture as a potential factor that could impact carbon isotopic ratios. Research has shown that soil texture has the ability to alter $\delta^{13}\text{C}$ values due to the unconsolidated form of sand which allows for the permeation of small-sized carbon particles, where it aids in the prevention of degradation of the element (Bird et al. 2000). In this study, we did not consider fire intensity, time length, or temperature, but these components have been shown to influence carbon isotopic signatures which should be considered in the future (Saito et al. 2007).

Although there is no statistical significance in pre-fire and post-fire samples collected within the immediate site, $\delta^{15}\text{N}$ ratios are enriched in soil A horizons. Specifically, there is

noticeable nitrogen enrichment in upland and transition zones, with the exception being near the wetland edge (Figure 5). In contrast, the chronic site shows nitrogen depletion. Knoepp et al. (2015) found $\delta^{15}\text{N}$ enrichments throughout a soil profile after a prescribed fire but discussed that the changes could be related to N_2 fixation. The $\delta^{15}\text{N}$ enrichment found in our study could also be due to the residual volatilization of material (Saito 2007) or the decomposition of organic matter (Craine et al. 2015). Both immediate and chronic sites are N limited but it was difficult to determine if nitrogen isotopic ratios differences are attributed to total N pools. Because both sites undergo fire regimes, deposited ash layers can add available nitrogen to the system which can then be either volatilized or absorbed by growing vegetation (McNaughton et al. 1998; Strydom et al. 2019). Studies have shown that disturbance can alter organic matter which affects nitrogen signature where removal can cause enrichment while the opposite can result in depletion (Hogberg 1997; Knoepp et al. 2015). A disturbance such as forest fires, can intake the depleted $\delta^{15}\text{N}$ surface layer leaving plants no choice but to extract N from lower horizons, which can affect and cause an enrichment in nitrogen isotopic ratios of plants (Hogberg 1997). Future studies could investigate the effects that fire intensity has on nitrogen isotopic signatures because variations could exist due to temperature differences (Czimczik et al. 2002; Certini 2011). Future studies could also study the effects that low-intensity fires have on microbial biomass which can alter $\delta^{15}\text{N}$ values.

3.6. Conclusion

Extensive research has been done on prescribed fire effects to forest soils regarding impacts to soil properties, hydrological properties, and nutrient dynamics separately, but few have investigated affects along a slope gradient in forested geographically isolated wetland watersheds. In this study, prescribed fire affects to unsaturated hydraulic conductivity, water

repellency, soil properties, nutrient pools (specifically total C, P, K, Mn, Fe, Ca, Mg, Al), and carbon and nitrogen isotopic ratios were investigated along a slope gradient in a forested geographically isolated wetland watershed. We analyzed samples collected at the immediate site under pre-fire and post-fire/post-rainfall conditions and compared it to the chronic site that was treated with fire approximately one year prior. We found no significant spatial differences in hydrological properties in our immediate watershed, but we did see temporal changes. We also found no prominent effects to soil properties, in terms of soil texture and bulk density, resulting from the fire in either watershed which suggests that the prescribed fires over time have been managed well in terms of intensity.

There are significant temporal nutrient changes between the immediate and chronic watershed within the A (in total P, K, Mn, Fe, Mg, and Al concentrations) and B (in P, K, Mg, Fe, and Al content) horizons as well as positive correlations (total K and Mg) existing in post-fire/post-rainfall condition. The significant differences in the horizons and higher nutrient levels present in our chronic site we interpret as related to the addition of ash (burned biomass) into the system over multiple years of burning. The observed differences in total C, Mn, and Al within sites, paired by sampling locations, in the A horizons and total Mn in the B horizons were significant, which could be caused by rain infiltration, the fire, or both. Interestingly, after the large rain event, we found that total Al and Fe concentrations were low in subsurface horizons within the chronic site, in contrast our immediate site showed high levels which we suggest is an immediate response to the prescribed fire. There are also observable temporal changes after the fire where potential nutrient losses could exist in upland and transition zone regions in relation to the observed nutrient increase (total C, P, Mg, K, Ca, and Mn) found along the wetland edge.

Alterations to carbon and nitrogen isotopic ratios are significant between sites and varied. In our immediate site after the fire, there are enrichments to carbon isotopic ratios found in the soil A horizon which has been discussed as potentially being caused by rainfall or ash inputs by other researchers. In the immediate site, after the fire, there are also short-term temporal changes where we found enrichment to nitrogen isotopic ratios in the localities above the wetland edge of this study, which could have been altered by the prescribed fire or caused by changes to N₂ fixation.

Overall, a prescribed fire has the potential to affect hydrological properties, the lateral and vertical nutrient movement along a low-relief hillslope, as well as surface and subsurface carbon and nitrogen isotopic signatures, in mostly sandy soil types. The well-drained sandy soils found in both watersheds likely affects nutrient dynamics and hydrological properties because the high hydraulic conductivity allows for transport of nutrients. While we only attribute a few immediate effects of the prescribed fire over the period of our study, we expect long-term (annual to decadal) effects on soil characteristics due to the prescribed fire management regime.

Our study illustrated the complexity of understanding specific controls on soil characteristics, infiltration, and nutrient cycling in the shallow subsurface. To tease out the subtle short-term changes, we recommend concentrated sampling of infiltration, water repellency, and soil moisture. Improved understanding of long-term impacts will ultimately require repeat sampling -before a burn, immediately after a burn, and after a large rain event- over multiple prescribed fire cycles. Further research into the impacts of fire within southeastern pine forests, and GIW systems in particular, is critical as climate change increases the potential risk of wildfire in the region. Understanding how these systems cycle and store nutrients will help us manage and protect these ecosystems.

3.7. References

- Alcañiz, M., Outeiro, L., Francos, M., Farguell, J., Úbeda, X., 2016, Long-term dynamics of soil chemical properties after a prescribed fire in a Mediterranean forest (Montgrí Massif, Catalonia, Spain), *Science of the Total Environment*, v. 572, p. 1329–1335.
- Alcañiz, M., Outeiro, L., Francos, M., Úbeda, X., 2018, Effects of prescribed fires on soil properties: a review, *Science of the Total Environment*, v. 613–614, p. 944–957.
- Ale R., Zhang L., Li X., Raskoti B.B., Pugnaire F.I., and Luo T., 2018, Leaf $\delta^{13}\text{C}$ as an indicator of water availability along elevation gradients in the dry Himalayas, *Ecological Indicators*, v. 94, p. 266-273.
- Badia-Villas, D., Esteban- Piñeiro, J., Girona-Garcia, A., Ortiz- Perpiñá, O., and Poch, R.M., 2020, Topsoil microstructure changes after a shrubland prescribed burn (Central Pyrenees, NE Spain), *Science of the Total Environment*, v. 748, p. 1-11.
- Balesdent, J.; Girardin, C., Mariotti, A., 1993, Site-related $\delta^{13}\text{C}$ of tree leaves and soil organic matter in a temperate forest, *Ecology*, v. 74, p. 1713–1721.
- Baniya, B., Bigelow, S.W., Sharma, A., Taylor, S., Vogel, J.G., Brantley, S.T., 2022, Re-Assembly of the longleaf pine ecosystem: effects of groundcover seeding on understory community, *Fire Behavior, and Soil Properties, Forests*, v. 13, no. 519, p. 1-17, <https://doi.org/10.3390/f13040519>
- Battle, J., and Golladay, S.W., 2003, Prescribed fire's impact on water quality of depressional wetlands in southwestern Georgia, *The American Midland naturalist*, v.150, no.1, p. 15-25.
- Bird, M.I., Veenendaal, E.M., Moyo, C., Lloyd, J., and Frost, P., 2000, Effect of fire and soil texture on soil carbon in a sub-humid savanna (Matopos, Zimbabwe), *Geoderma*, v. 94, no.1, p. 71-90.
- Birkeland, P. W., 1999, *Soils and Geomorphology*, 3rd ed., 128 pp., Oxford Univ. Press, New York.
- Boring, L.R., Hendricks, J.J., Wilson, C.A., and Mitchell R.J., 2004, Season of burn and nutrient losses in a longleaf pine ecosystem, *International Journal of Wildland Fire*, v.13, p. 443–453, doi:10.1071/WF03060
- Boyer, W.D., and Miller, J.H., 1994, Effect of burning and brush treatments on nutrient and soil physical properties in young longleaf pine stands, *Forest Ecology and Management*, v. 70 p.311-318.
- Brady, N.C. and Weil, R.R., 2008, *The nature and properties of soil*, 14 ed. Prentice-Hall, Upper Saddle River, New Jersey.

- Butnor, J.R., Johnsen, K.H., Maier, C.A., and Nelson, C.D., 2020, Intra-annual variation in soil C, N and nutrients pools after prescribed fire in a Mississippi longleaf pine (*Pinus palustris* Mill.) plantation, *Forests*, v. 11, no.2, p. 181.
- Certini, G., Nocentini, C., Knicker, H., Afioli, P., and Rumpel, C., 2011, Wildfire effects on soil organic matter quantity and quality in two fire-prone Mediterranean pine forests, *Geoderma*, v. 167-168, p. 148–155.
- Chief, K., Young, M.H., and Shafer, D.S., 2012, Changes in soil structure and hydraulic properties in a wooded-shrubland ecosystem following a prescribed fire, *Soil Science Society of America Journal*, p. 1965-1977.
- Christensen, N. L., 1977, Fire and soil-plant nutrient relations in a pine-wiregrass savanna on the coastal plain of North Carolina, *Oecologia*, v. 31, p. 27–44.
- Coates, T.A., Hagan D.L., Aust, W.M., Johnson A., Keen J.C., Chow A.T., and Dozier J.H., 2018, Mineral Soil Chemical Properties as Influenced by Long-Term Use of Prescribed Fire with Differing Frequencies in a Southeastern Coastal Plain Pine Forest, *Forests*, v.9, no. 12, p. 1-14.
- Collins, S.L., Knapp, A.K., Briggs, J.M., Blair, J.M., Steinaur, E.M., 1998, Modification of diversity by grazing and mowing in native tallgrass prairie, *Science*, v. 280, p. 745–747.
- Craine, J.M., Brookshire, E.N.J., Cramer, M.D., Hasselquist, N.J., Koba, K., Marin-Spiotta, E., Wang, L., 2015, Ecological interpretations of nitrogen isotope ratios of terrestrial plants and soils, *Plant Soil*, v. 396, p. 1–26.
- Czimczik, C.I., Preston, C.M., Schmidt, M.W.I., Werner, R.A., Schulze, E.D., 2002, Effects of charring on mass, organic carbon, and stable carbon isotope composition of wood, *Organic Geochemistry* 33, v. 33, p. 1207–1223.
- DeBano, L.F., and Krammes, J.S., 1966, Water repellent soils and their relation to wildfire temperatures, *International Association of Scientific Hydrology, Bulletin*. no. 11, p. 14–19, doi:10.1080/02626666609493457
- De Marco, A., Gentile, A.E., Arena, C., and De Santo, A.V., 2005, Organic matter, nutrient content and biological activity in burned and unburned soils of a Mediterranean maquis area of southern Italy, *International Journal of Wildland Fire*, v. 14, p. 365–377.
- Environmental Protection Agency, U. S., 1996, Method 6010B: Inductively coupled plasma-atomic emission spectrometry, SW-846 test methods for evaluating solid wastes.
- Fowler, C., and Konopik, E., 2007, The history of fire in the southern United States, *Human Ecology Review*, v. 14, no. 2, p. 165-176.

- Gonzalez Parra, J., Cala Rivero, V., and Iglesias Lopez, T., 1996, Forms of Mn in soils affected by a forest fire, *The Science of the Total Environment*, v. 181, p. 231-236.
- González-Pelayo, O., Andreu, V., Gimeno-García, E., Campo, J., Rubio, J., 2010, Effects of fire and vegetation cover on hydrological characteristics of a mediterranean shrub-land soil, *Hydrological Processes*, v. 24, p. 1504–1513.
- Grayson, R.B., Western, A.W., Chiew, F.H.S., and Bloschl, G., 1997, Preferred states in spatial soil moisture patterns: Local and nonlocal controls, *Water Resources Research*, v. 33, no. 12, p. 2897–2908.
- Heathcote, A. J., and Downing, J. A., 2012, Impacts of eutrophication on carbon burial in freshwater lakes in an intensively agricultural landscape. *Ecosystems*, v. 15, no. 1, p. 60-70.
- Högberg, P., 1997, Tansley Review No. 95. ^{15}N natural abundance in soil-plant systems, *New Phytologist*, v. 137, no. 2, p. 179–203.
- Hallett, P.D., Baumgartl, T., and Young, I.M., 2001, Subcritical water repellency of aggregates from a range of soil management practices, *Soil Science Society of America Journal*, v. 65, p. 184–190.
- Hillel, D., 2004, *Introduction to Environmental Soil Physics*, Elsevier Academic Press, Amsterdam.
- Holland, A.M., Rutledge, B.T., Jack, S.B., and Stober, J.M., 2019, The longleaf pine forest: long-term monitoring and restoration of a management dependent ecosystem, *Journal for Nature Conservation*, v. 47, p. 38-50.
- Huffman, E.L., MacDonald, L.H., and Stednick, J.D., 2001, Strength and persistence of fire-induced soil hydrophobicity under ponderosa and lodgepole pine, *Colorado Front Range, Hydrological Processes*, v. 15, p. 2877–2892, doi:10.1002/hyp.379
- Jansen, L.S., Pierre, S., and Boughton, E.H., 2019, Interactions of fire, grazing and pasture management: short-term and long-term responses of water quality to management regimes in subtropical isolated wetlands, *Agriculture, Ecosystems and Environment*, v. 280, p. 102-113.
- JMP®, version 16.0, SAS Institute Inc., Cary, NC, 1989-2021.
- Knoepp, J.D.; Taylor, S.R.; Boring, L.R.; Miniati, C.F., 2015, Influence of forest disturbance on stable nitrogen isotope ratios in soil and vegetation profiles, *Soil Science Society of America Journal*, v. 79, no. 5, p. 1470–1481.
- Kennard, D.K., Gholz, H., 2001, Effects of high-and low-intensity fires on soil properties and plant growth in a Bolivian dry forest, *Plant Soil*, v. 234, p. 119–129.

- Kirkman, L.K., Mitchell, R.J., Helton, R.C., and Drew, M.B., 2001, Productivity and species richness across an environmental gradient in a fire-dependent ecosystem, *American Journal of Botany*, v. 88, p. 2119-2128.
- Kirkman, L.K.; Jack, S.B., 2017, *Ecological restoration and management of Longleaf pine forests*, CRC Press: Boca Raton, FL, USA.
- Lafon, C.W., 2010, Fire in the american south: vegetation impacts, history, and climatic relations, *Geography Compass*, v. 4, no.8, p. 919–944, 10.1111/j.1749-8198.2010.00363.x
- Lavoie, M., Starr, G., Mack, MC., Martin, T.A., and Gholz, H.L., 2010, Effects of a prescribed fire on understory vegetation, carbon pools, and soil nutrients in a longleaf pine-slash pine forest in Florida, v. 30, no. 1, *Natural Areas Journal*, p. 82-94.
- Lichner, L., Hallett, P.D., Feeney, D.S., Dugova, O., Sir, M., and Tesar, M., 2007, Field measurement of soil water repellency and its impact on water flow under different vegetation, *Biologia, Bratislava*, v. 62, no. 5, p. 537–541.
- McKee, W.H., 1982, Changes in soil fertility following prescribed burning on costal pine sites, United States Department of Agriculture Forest Service Research Paper SE-234.
- McNaughton, S.J., Stronach, N.R.H., Georgiadis, N.J., 1998, Combustion in natural fires and global emissions budgets, *Ecological Applications*, v. 8, p. 464–468.
- METER Group Inc. 2001, USA., WA.
- Miller, W.P. and Miller, D.M., 1987, A micro-pipette method for soil mechanical analysis, *Communications in Soil Science & Plant Analysis*, v. 18, p. 1–15.
- Mills, A.J., Fey, M.V., 2004, Frequent fires intensify soil crusting: physicochemical feedback in the pedoderm of long-term burn experiments in South Africa, *Geoderma*, v. 12, no. 1-2, p. 45–64.
- Mitchell, R.J., Palik, B.J., Hunter, M.L., 2002, Natural disturbance as a guide to silviculture, *Forest Ecology and Management*, v.155, p. 315–317.
- Moyo, C.S., Frost, P.G.H., Campbell, B.M., 1998, Modification of soil nutrients and microclimate by tree crowns in semi-arid rangeland of South-Western Zimbabwe, *African Journal of Range and Forage Science*, v. 15, p. 16–22.
- Neary, D.G., Ryan, K.C., and DeBano, L.F., editors. 2005, *Wildland fire in ecosystems: Effects of fire on soil and water*, RMRS-GTR-42, v. 4, U.S. Forest Service, Rocky Mountain Research Station, Ogden, UT.

- Park, B.B., Yanai, R.D., Sahm, J.M., Lee, D.K., and Abrahamson, L.P., 2005, Wood ash effects on plant and soil in a willow bioenergy plantation, *Biomass and Bioenergy*, v. 28, p. 355–365.
- Pereira, P., Ubeda, X., Martin, D., Mataix-Solera, J., and Guerrero, C., 2011, Effects of a low severity prescribed fire on water-soluble elements in ash from a cork oak (*Quercus suber*) forest located in the northeast of the Iberian Peninsula, *Environmental Research*, v. 111, p. 237–247.
- Rau, B.M., Johnson, D.W., Blank, R.R., Chambers, C., 2009, Soil carbon and nitrogen in a Great Basin pinyon–juniper woodland: influence of vegetation, burning, and time, *Journal of Arid Environments*, v. 73, p. 472–479.
- Richter, D. D., Ralston, C. W., and Harms W.R., 1982, Prescribed fire: effects on water quality and forest nutrient cycling, *Science*, no. 4533, vol. 215, p. 661-663.
- Rooij, G.H., 1995, A three-region analytical model of solute leaching in a soil with a water-repellent top layer, *Water Resources Research*, v. 31, no.11, p. 2701-2707.
- Robichaud, P., Wagenbrenner, J., Brown, R., Wohlgemuth, P., Beyers, J., 2008, Evaluating the effectiveness of contour-felled log erosion barriers as a post-fire runoff and erosion mitigation treatment in the western United States, *International Journal of Wildland Fire*, v. 17, p. 255–273.
- Saito, L., Miller, W.W., Johnson, D.W., Qualls, R.G., Provencher, L., Carroll, E., and Szameitat, P., 2007, Fire effects on stable isotopes in a sierran forested watershed, *Journal of Environmental Quality*, v. 36, p. 91-100.
- SAS Institute Inc. 2008, JMP® 8 Statistics and Graphics Guide, Volumes 1 and 2, Cary, NC: SAS Institute Inc.
- Savadogo, P., Sawadogo, L., Tiveau, D., 2007, Effects of grazing intensity and prescribed fire on soil physical and hydrological properties and pasture yield in the savanna woodlands of Burkina Faso, *Agriculture, Ecosystems, Environment*, v. 118, p. 80–92.
- Savage, SM., 1974, Mechanism of fire-induced water repellency in soil, *Soil Science Society of America, Proceedings*, v. 38, p. 652-657.
- Schafer, J.L., Breslow, B.P., Just, M.G., Hohmann, M.G., Hollingsworth, S.N., Swatling-Holcomb, S.L., and Hoffman, W.A., 2013, Current and historical variation in wiregrass (*Aristida stricta*) abundance and distribution is not detectable from soil $\delta^{13}\text{C}$ measurements in longleaf pine (*Pinus palustris*) savannas, *Castanea*, v. 78, no.1, p. 28–36.

- Scharenbroch B.C., Nix B., Jacobs K.A., and Bowles M.I., 2012, Two decades of low-severity prescribed fire increases soil nutrient availability in a Midwestern, USA oak (*Quercus*) forest, *Geoderma*, v. 183-184, p. 80-91.
- Soil Survey Staff, Natural Resources Conservation Service, United States Department of Agriculture. Web Soil Survey. Available online at the following link: <http://websoilsurvey.sc.egov.usda.gov/>. Accessed [07/31/2022].
- Stieglitz, M., Shaman, J., McNamara, J., Engel, V., Shanley, J., and Kling, G.W., 2003, An approach to understanding hydrologic connectivity on the hillslope and the implications for nutrient transport, *Global Biogeochemical Cycles*, v.17, no. 4, p. 16-1-16-15, doi:10.1029/2003GB002041
- Stoof, C.R., Moore, D., Ritsema, C.J., Dekker, L.W., 2011, Natural and fire-induced soil water repellency in a Portuguese shrubland, *Soil Science Society of America*, v. 75, p. 2283–2295.
- Storer, D.A., 1984, A simple high sample volume ashing procedure for determination of soil organic matter, *Communications in Soil Science and Plant Analysis*, v. 7, no. 15, p.759-772, DOI: 10.1080/00103628409367515
- Strydom, T., Riddell, E.S., Rowe, T., Govender, N., Lorentz, S.A., le Roux P.A.L., and Wigley-Coetsee C., 2019, The effect of experimental fires on soil hydrology and nutrients in an African savanna, *Geoderma*, v. 345, p. 114–122, <https://doi.org/10.1016/j.geoderma.2019.03.027>
- Tahmasbian I., Xu Z., Nguyen T.T.N., Che R., Omidvar N., Lambert G., and Bai S.H., 2019, Short-term carbon and nitrogen dynamics in soil, litterfall and canopy of a suburban native forest subjected to prescribed burning in subtropical Australia, *Journal of Soils and Sediments*, v. 19, p. 3969-3981.
- Verma S., and Jayakumar S., 2012, Impact of forest fire on physical, chemical and biological properties of soil: A review, *Proceedings of the International Academy of Ecology and Environmental Sciences*, v. 2, no. 3, p. 168-176.
- Wells, C. G., 1971, Effects of prescribed burning on soil chemical properties and nutrient availability, In *Proceedings Prescribed Burning Symposium*, v.1971, p. 86-97.

APPENDIX A: SOIL PROPERTIES

A.1. Soil Descriptions

Table A1. Soil description from upland region before the prescribed fire retrieved from immediate site.

Auger #	Depth (cm)	Soil Color	Horizon	Soil Texture (Determined through USDA Calculator)
A1	0-15	10 YR 4/1 Dark Gray	A	Loamy Sand
A2	15-28	10 YR 5/4 Yellowish Brown	AB	Loamy Sand
A3	28-35	10 YR 6/4 Light Yellowish Brown	Bw	Sandy Clay Loam
A4	35-43	10 YR 7/6 Yellow	Bt	Sandy Clay
A5	43-59	10 YR 6/6 Brownish Yellow	Bt	Sandy Clay

Table A2. Description of soil samples collected from transition zone 1 before the scheduled prescribed fire in immediate site.

Auger #	Depth (cm)	Soil Color	Horizon	Soil Texture (Determined through USDA Calculator)
B1	0-19	10 YR 3/2 Very Dark Grayish Brown	A	Loamy Sand
B2	19-29	<i>First Half</i> 10YR 4/2 Dark Grayish Brown <i>Second Half</i> 10 YR 5/4 Yellowish Brown	AB	Loamy Sand
B3	29-40	10 YR 5/4 Yellowish Brown Possible redox feature	Bw or Bt	Loamy Sand
B4	40-50	7.5 YR 6/6 Reddish Yellow	Bt	Sandy Clay Loam
B5	50-57	7.5 YR 7/6 Reddish Yellow	Bt	Sandy Clay Loam

Table A3. Soil description of soil core collected in immediate site from transition zone 2 before the prescribed fire.

Auger #	Depth (cm)	Soil Color	Horizon	Soil Texture (Determined through USDA Calculator)
C1	0-19	10 YR 3/1 Very Dark Gray	A	Loamy Sand
C2	19-34	10 YR 4/2 Dark Grayish Brown	Bw	Loamy Sand
C3	34-49	10 YR 6/3 Pale Brown	Bw	Loamy Sand
C4	49-55	10 YR 6/3 Pale Brown	Bw	Sandy Loam

Table A4. Description of samples collected from wetland edge before the prescribed fire in immediate site.

Auger #	Depth (cm)	Soil Color	Horizon	Soil Texture (Determined through USDA Calculator)
D1	0-25	10 YR 3/1 Very Dark Gray	A	Loamy Sand
D2	25-47	10 YR 6/1 Gray	B	Loamy Sand

Table A5. Soil description from upland areas after the prescribed fire retrieved on 06/25/2021.

Auger #	Depth (cm)	Soil Color	Horizon	Soil Texture (Determined through USDA Calculator)
A1	0-16	10 YR 3/1 Very Dark Gray	A	Loamy Sand
A2	16-31	10 YR 4/2 Dark Grayish Brown	AB	Loamy Sand
A3	31-43	10 YR 5/4 Yellowish Brown	Bt	Sandy Loam
A4	43-55	10 YR 6/4 Light Yellowish Brown	Bt	Sandy Clay Loam

Table A6. Description of soil samples collected from transition zone 1 after the scheduled prescribed fire retrieved on 06/25/2021 in immediate site.

Auger #	Depth (cm)	Soil Color	Horizon	Soil Texture (Determined through USDA Calculator)
B1	0-15	10 YR 3/2 Brown	A	Loamy Sand
B2	15-29	<i>First Half</i> 10 YR 4/2 Dark Grayish Brown <i>Second Half</i> 10 YR 5/4 Yellowish Brown	AB	Loamy Sand
B3	29-46	10 YR 5/6 Yellowish Brown	Bt	Sandy Loam
B4	46-52	7.5 YR 5/6 Strong Brown	Bt	Sandy Clay Loam

Table A7. Soil description of soil core collected from transition zone 2 after the prescribed fire retrieved on 06/25/2021 in immediate site.

Auger #	Depth (cm)	Soil Color	Horizon	Soil Texture (Determined through USDA Calculator)
C1	0-20	10 YR 3/1 Very Dark Gray	A	Loamy Sand
C2	20-37	10 YR 4/2 Dark Grayish Brown	A	Loamy Sand
C3	37-47	10 YR 5/4 Yellowish Brown	Bt	Sandy Loam
C4	47-67	7.5 YR 6/4 Light Brown	Bt	Sandy Clay Loam

Table A8. Description of samples collected from wetland edge after the scheduled prescribed fire retrieved on 06/25/2021 in immediate site.

Auger #	Depth (cm)	Soil Color	Horizon	Soil Texture (Determined through USDA Calculator)
D1	0-16	10 YR 2/1 Black	A	Loamy Sand
D2	16-24	10 YR 4/2 Dark Grayish Brown	A	Loamy Sand
D3	24-47	10 YR 5/4 Yellowish Brown	Bt	Sandy Loam

Table A9. Soil description of samples from chronic site upland region collected on 05/11/2021.

Auger #	Depth (cm)	Soil Color	Horizon	Soil Texture (Determined through USDA Calculator)
E1	0-17	10 YR 3/1 Very Dark Gray	A	Loamy Sand
E2	17-27	10 YR 4/2 Dark Grayish Brown	B	Sandy Loam
E3	27-36	10 YR 5/4 Yellowish Brown	B	Sandy Loam
E4	36-44	10 YR 5/6 Yellowish Brown	B	Sandy Clay Loam

Table A10. Description of samples retrieved from chronic site in transition zone 1 collected on 05/11/2021.

Auger #	Depth (cm)	Soil Color	Horizon	Soil Texture (Determined through USDA Calculator)
F1	0-14	10 YR 3/2 Brown	A	Loamy Sand
F2	14-24	10 YR 4/3 Brown	Bt	Sandy Loam
F3	24-34	10 YR 5/4 Yellowish Brown	Bt	Sandy Loam
F4	34-44	10 YR 6/6 Brownish Yellow	Bt	Sandy Clay Loam

Table A11. Soil description of samples retrieved from chronic site in transition zone 2 collected on 05/11/2021.

Auger #	Depth (cm)	Soil Color	Horizon	Soil Texture (Determined through USDA Calculator)
G1	0-18	10 YR 3/1 Very Dark Gray	A	Loamy Sand
G2	18-27	<u>First Half:</u> 10 YR 3/2 Very Dark Grayish Brown <u>Second Half:</u> 10 YR 5/3 Brown	AB	Sandy Loam
G3	27-35	7.5 YR 4/4 Brown	Bw or Bt	Sandy Clay Loam
G4	35-43	7.5 YR 5/6 Strong Brown	Bw or Bt	Sandy Clay Loam

Table A12. Description of soil samples collected from chronic site point retrieved from wetland edge on 05/11/2021.

Auger #	Depth (cm)	Soil Color	Horizon	Soil Texture (Determined through USDA Calculator)
H1	0-18	10 YR 3/1 Very Dark Gray	A	Loamy Sand
H2	18-33	10 YR 4/2 Dark Grayish Brown	Bt	Sandy Loam
H3	33-49	2.5 YR 4/6 Red Redox feature 10 YR 6/6 Brownish Yellow	Bt	Sandy Loam
H4	49-64	10 YR 6/6/ Brownish Yellow 2.5 YR 4/6 Red Redox Feature	Bt	Sandy Clay Loam

Table A13. Soil description of samples from chronic site in upland area retrieved on 06/25/2021.

Auger #	Depth (cm)	Soil Color	Horizon	Soil Texture (Determined through USDA Calculator)
E1	0-17	10 YR 3/1 Very Dark Gray	A	Loamy Sand
E2	17-26	10 YR 5/4 Yellowish Brown	AB	Sandy Loam
E3	26-39	7.5 YR 5/6 Strong Brown	Bt	Sandy Clay Loam

Table A14. Description of samples retrieved from chronic site in transition zone 1 collected on 06/25/2021.

Auger #	Depth (cm)	Soil Color	Horizon	Soil Texture (Determined through USDA Calculator)
F1	0-10	10 YR 2/1 Black	A	Loamy Sand
F2	10-25	10 YR 4/2 Dark Grayish Brown	A	Sandy Loam
F3	25-40	10 YR 6/4 Light Yellowish Brown	Bt	Sandy Loam
F4	40-52	10 YR 6/6 Brownish Yellow	Bt	Sandy Clay Loam

Table A15. Soil description of samples retrieved from chronic site in transition zone 2 collected on 06/25/2021.

Auger #	Depth (cm)	Soil Color	Horizon	Soil Texture (Determined through USDA Calculator)
G1	0-15	10 YR 3/1 Very Dark Gray	A	Loamy Sand
G2	15-27	10 YR 5/3 Brown	AB	Sandy Loam
G3	27-36	7.5 YR 5/6 Strong Brown	Bt	Sandy Clay Loam
G4	36-45	7.5 YR 6/6 Reddish Yellow	Bt	Sandy Clay Loam

Table A16. Description of soil samples collected from chronic site point retrieved from wetland edge on 06/25/2021.

Auger #	Depth (cm)	Soil Color	Horizon	Soil Texture (Determined through USDA Calculator)
H1	0-16	10 YR 3/1 Very Dark Gray	A	Loamy Sand
H2	16-33	10 YR 5/3 Brown	AB	Sandy Loam
H3	33-51	10 YR 6/4 Light Yellowish Brown	Bt	Sandy Loam
H4	51-65	10 YR 6/4 Light Yellowish Brown	Bt	Sandy Loam

A.2. Bulk Density

Table A17. Bulk density calculations from samples in immediate and chronic sites.

Site	Sample Collection Date	Sampling Point	Bulk Density (g/cm ³)
Upland	5/10/2021	A	0.1827
Transition Zone 1	5/10/2021	B	0.1840
Transition Zone 2	5/10/2021	C	0.2316
Wetland Edge	5/10/2021	D	0.4247
Upland	5/11/2021	E	0.1072
Transition Zone 1	5/11/2021	F	0.1936
Transition Zone 2	5/11/2021	G	0.2012
Wetland Edge	5/11/2021	H	0.3834
Upland	6/25/21	A	0.1837
Transition Zone 1	6/25/21	B	0.1795
Transition Zone 2	6/25/21	C	0.1751
Wetland Edge	6/25/21	D	0.1670
Upland	6/25/21	E	0.1352
Transition Zone 1	6/25/21	F	0.2081
Transition Zone 2	6/25/21	G	0.1617
Wetland Edge	6/25/21	H	0.1818

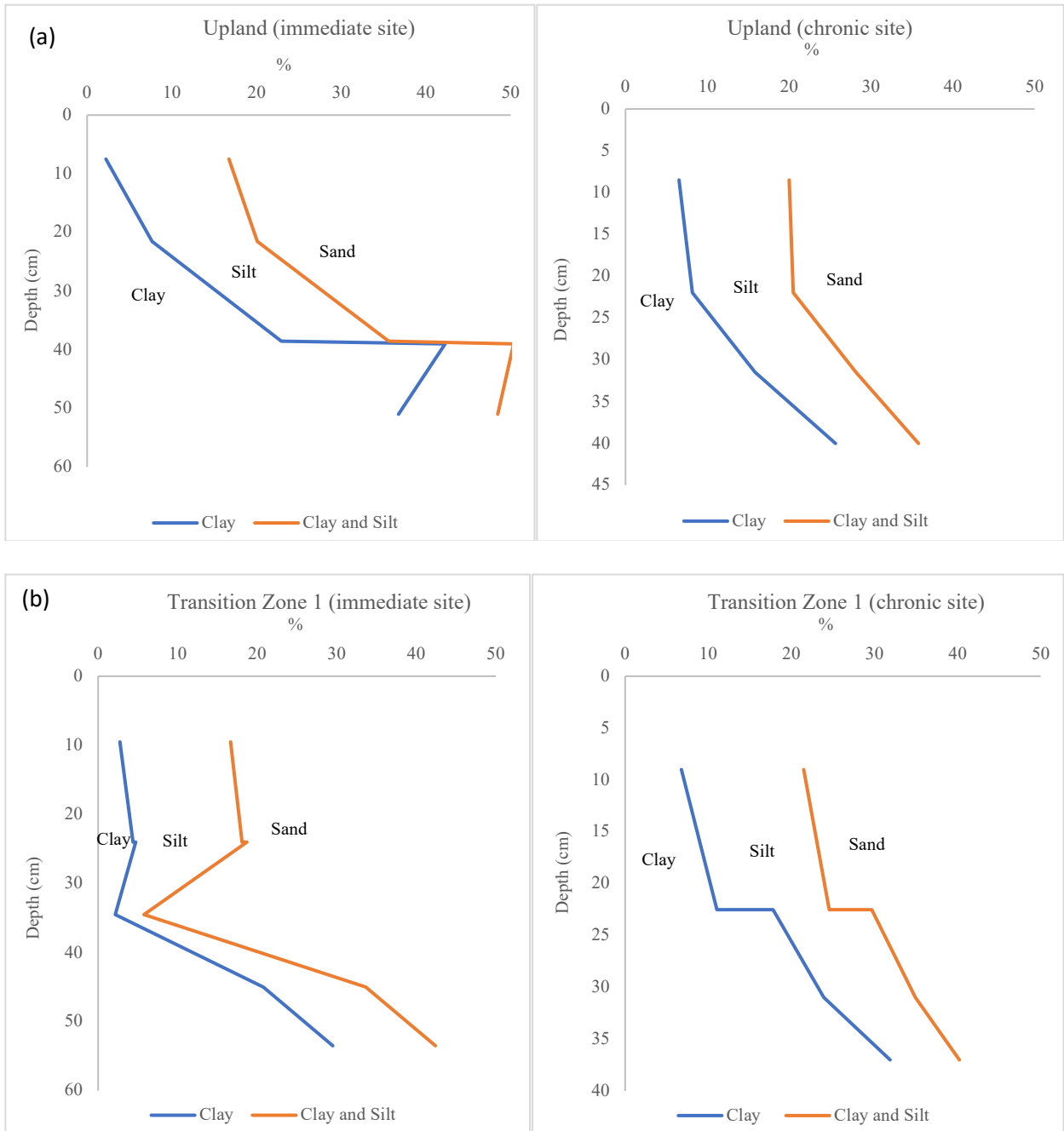
Table A18. Two-way ANOVA analysis for bulk density within samples (sampling times) and between sites (columns).

	SS	df	MS	F	P-value	F crit
Sample (Sampling times)	0.016662125	1	0.016662125	2.406822264	0.146769438	4.747225347
Columns (Sites)	0.001522391	1	0.001522391	0.219907384	0.64751531	4.747225347

Table A19. Unpaired t-test results for the differences in bulk density before and after rain event (before minus after).

	Immediate	Chronic
Mean	0.079417706	0.049664146
Variance	0.014795075	0.011110164
df	6	
t Stat	0.369721861	
P(T<=t) one-tail	0.362144119	
t Critical one-tail	1.943180281	
P(T<=t) two-tail	0.724288238	
t Critical two-tail	2.446911851	

A.3. Grain Size Analysis



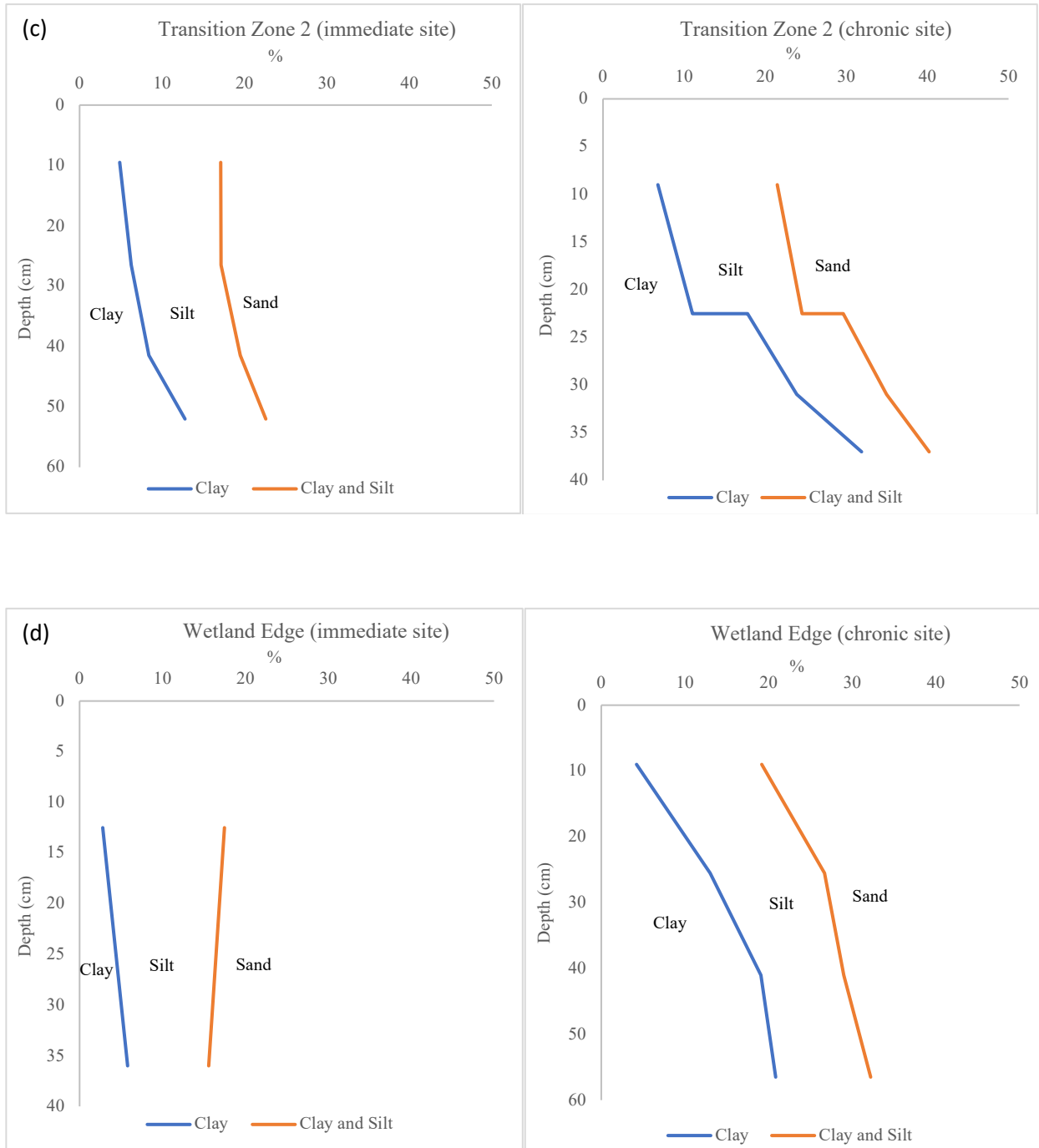
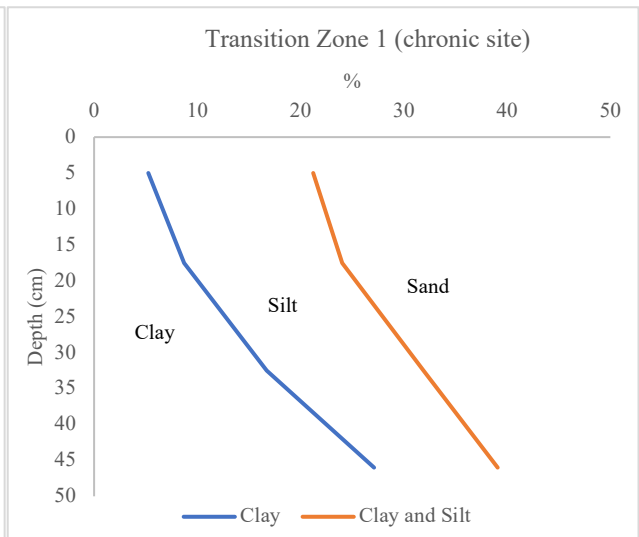
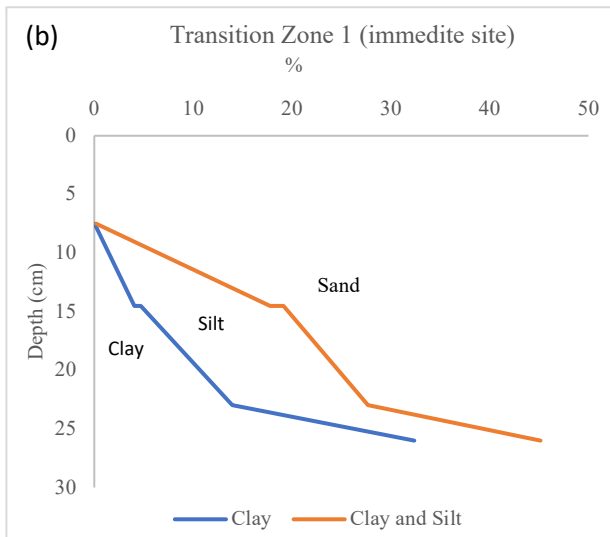
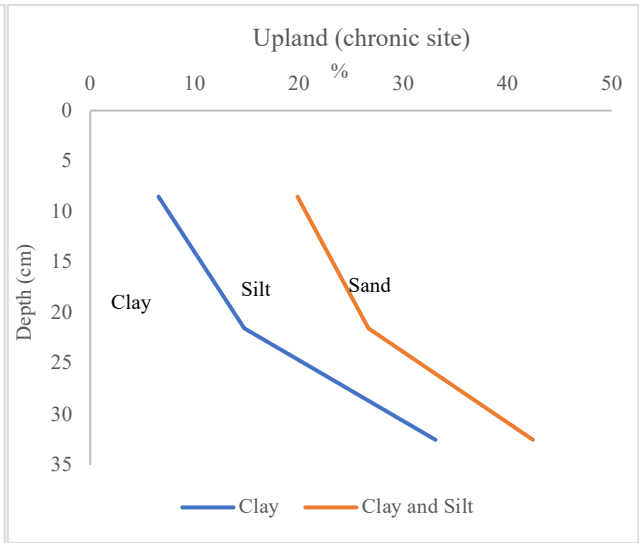
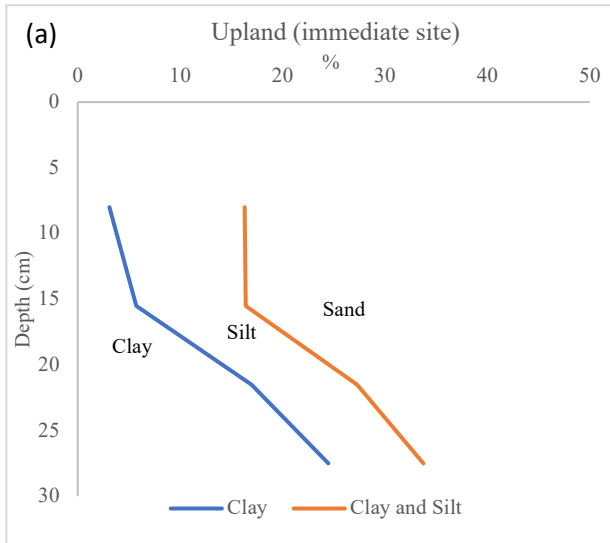


Figure A1. Grain size distribution of clay (blue line) and clay in combination with silt (orange line) in upland (a), transition zone 1 (b), transition zone 2 (c), and wetland edge comparison between cores taken before the rain event (sampling time 1) from immediate and chronic sites.



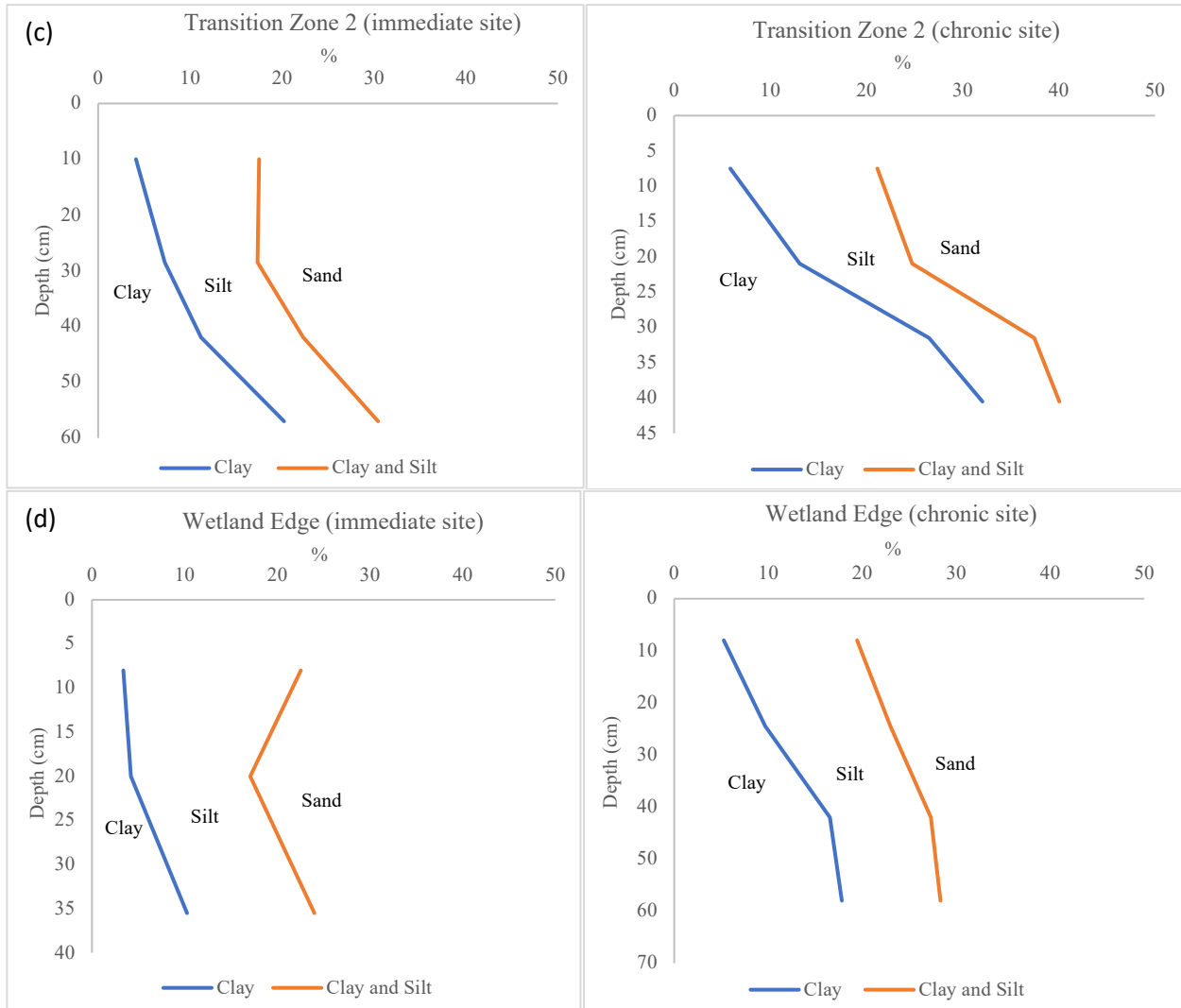


Figure A2. Grain size distribution of clay (blue line) and clay in combination with silt (orange line) in upland (a), transition zone 1 (b), transition zone 2 (c), and wetland edge comparison between cores taken after the rain event (sampling time 2) from immediate and chronic sites.

Table A20. Sampling time 1 grain size analysis data in immediate and chronic sites.

	Depth	Sand	Silt	Clay
<u>Point A</u>				
	0-15	83.0977	14.5235	2.2179
	15-28	79.8395	12.4393	7.6777
	28-35	63.6046	12.6922	22.9024
	35-43	49.4863	8.0861	42.2685
	43-59	51.2906	11.7715	36.7351
<u>Point B</u>				
	0-19	83.2679	13.8918	2.7616
	19-29	81.8939	13.7064	4.3897
	19-29	81.2358	13.9391	4.7651
	29-40	76.3822	14.7985	8.8193
	40-50	66.3280	12.8621	20.8043
	50-57	57.5836	12.9092	29.5073
<u>Point C</u>				
	0-19	82.6007	12.2502	4.8664
	19-34	82.7859	10.8939	6.2892
	34-49	80.2694	11.1252	8.3891
	49-55	77.3999	9.7995	12.7869
<u>Point D</u>				
	0-25	82.3225	14.6851	2.7922
	25-47	84.4116	9.7824	5.7950
<u>Point E</u>				
	0-17	79.5427	13.4650	6.5389
	17-27	79.2580	12.2800	8.1996
	27-36	71.7528	12.3536	15.8276
	36-44	63.9780	10.1459	25.6625
<u>Point F</u>				
	0-14	81.0927	14.5458	4.1158
	14-24	77.1674	14.8182	8.0095
	24-34	72.0041	13.8628	14.1269
	34-44	62.1081	11.5358	26.2431
<u>Point G</u>				
	0-18	78.3594	14.7167	6.7692
	18-27	75.4499	13.5034	11.0467
		70.1346	11.8583	17.7929
	27-35	65.0621	11.0189	23.9137
	35-43	59.7157	8.3308	31.8814
<u>Point H</u>				
	0-18	80.7131	14.9663	4.2147
	18-33	73.2151	13.7109	12.9907
	33-49	70.8575	9.9266	19.0917
	49-64	67.7083	11.3540	20.8470

Table A21. Sampling time 2 grain size analysis data for the immediate and chronic sites.

	Depth	Sand	Silt	Clay
<u>Point A</u>				
	0-16	83.6885	13.2072	3.0944
	16-31	83.4322	10.7277	5.6989
	31- 43	72.7176	10.2939	16.9832
	43-55	66.2482	9.2791	24.4705
<u>Point B</u>				
	0-15	81.0384	16.3295	2.5696
	15-29	82.2302	13.7249	4.0448
	15-29	80.8760	14.4504	4.6736
	29-46	72.2903	13.7300	13.9462
	46-52	54.7684	12.7684	32.3759
<u>Point C</u>				
	0-20	82.5159	13.3701	4.1139
	20-37	82.6604	10.0847	7.2549
	37-47	77.6728	11.1164	11.2108
	47-67	69.5469	10.2292	20.2240
<u>Point D</u>				
	0-16	77.4816	19.1315	3.3869
	16-24	82.8650	12.8696	4.2096
	24-47	75.9976	13.7440	10.2584
<u>Point E</u>				
	0-17	80.1198	13.3276	6.5445
	17-26	73.3167	11.8971	14.7792
	26-39	57.3515	9.3438	33.1029
<u>Point F</u>				
	0-10	78.7790	15.9688	5.2522
	10-25	75.9876	15.2986	8.7074
	25-40	67.9494	15.1795	16.7393
	40-52	60.9141	11.9711	27.1148
<u>Point G</u>				
	0-15	78.7246	15.2906	5.8505
	15-27	75.1382	11.7284	13.0554
	27-36	62.3984	10.9460	26.5291
	36-45	59.8693	7.9942	32.0674
<u>Point H</u>				
	0-16	80.3735	14.1846	5.2707
	16-33	76.9816	13.3162	9.7022
	33-51	72.6863	10.7210	16.5927
	51-65	71.6755	10.4964	17.8281

Table A22. Two-way ANOVA analysis for grain size in soil A horizon within samples (sampling times) and between sites (columns).

	SS	df	MS	F	P-value	F crit
Sand						
Sample (Sampling times)	4.280190589	1	4.280190589	1.759057767	0.209431733	4.747225347
Columns (Sites)	20.94994499	1	20.94994499	8.609935162	0.012504409	4.747225347
Silt						
Sample (Sampling times)	3.769085929	1	3.769085929	1.378853687	0.263073867	4.747225347
Columns (Sites)	0.053314281	1	0.053314281	0.01950409	0.891247564	4.747225347
Clay						
Sample (Sampling times)	0.203886624	1	0.203886624	0.192928854	0.668295145	4.747225347
Columns (Sites)	21.98118788	1	21.98118788	20.7998215	0.000653952	4.747225347

Table A23. Unpaired t-test results for the difference in grain size distribution in soil A horizon before and after the rain event (before minus after).

	Immediate	Chronic
Sand		
Mean	1.641121223	0.427740925
Variance	5.995933499	1.734353533
df	6	
t Stat	0.872828914	
P(T<=t) one-tail	0.208157582	
t Critical one-tail	1.943180281	
P(T<=t) two-tail	0.416315165	
t Critical two-tail	2.446911851	
Silt		
Mean	-1.671946518	-0.269466867
Variance	5.839441516	0.89787942
df	6	
t Stat	-1.080644746	
P(T<=t) one-tail	0.160682933	
t Critical one-tail	1.943180281	
P(T<=t) two-tail	0.321365866	
t Critical two-tail	2.446911851	
Clay		
Mean	-0.131711433	-0.319826632
Variance	0.551827303	0.947153594
df	6	
t Stat	0.307295241	
P(T<=t) one-tail	0.384502612	
t Critical one-tail	1.943180281	
P(T<=t) two-tail	0.769005224	
t Critical two-tail	2.446911851	

Table A24. Two-way ANOVA analysis for grain size in soil B horizon within samples (sampling times) and between sites (columns).

	SS	df	MS	F	P-value	F crit
Sand						
Sample (Sampling times)	14.48929399	1	14.48929399	0.348026193	0.566175633	4.747225347
Columns (Sites)	177.0883208	1	177.0883208	4.253580209	0.061507066	4.747225347
Silt						
Sample (Sampling times)	0.131529316	1	0.131529316	0.036185391	0.852313166	4.747225347
Columns (Sites)	0.248496057	1	0.248496057	0.068364432	0.798166887	4.747225347
Clay						
Sample (Sampling times)	13.16235701	1	13.16235701	0.315206974	0.58483518	4.747225347
Columns (Sites)	193.4505928	1	193.4505928	4.632679084	0.052421356	4.747225347

Table A25. Unpaired t-test results for the difference in grain size analysis in soil B horizon before and after the rain event (before minus after).

	Immediate	Chronic
Sand		
Mean	-1.016212268	4.822692794
Variance	64.00091218	47.08072474
df	6	
t Stat	-1.10800131	
P(T<=t) one-tail	0.155144993	
t Critical one-tail	1.943180281	
P(T<=t) two-tail	0.310289987	
t Critical two-tail	2.446911851	
Silt		
Mean	-0.605584471	0.242914765
Variance	6.910892323	3.730937432
df	6	
t Stat	-0.520203533	
P(T<=t) one-tail	0.310775194	
t Critical one-tail	1.943180281	
P(T<=t) two-tail	0.621550387	
t Critical two-tail	2.446911851	
Clay		
Mean	1.373034552	-5.001030833
Variance	34.13748719	72.76805044
df	6	
t Stat	1.23295268	
P(T<=t) one-tail	0.131852996	
t Critical one-tail	1.943180281	
P(T<=t) two-tail	0.263705991	
t Critical two-tail	2.446911851	

APPENDIX B: HYDROLOGICAL PROPERTIES

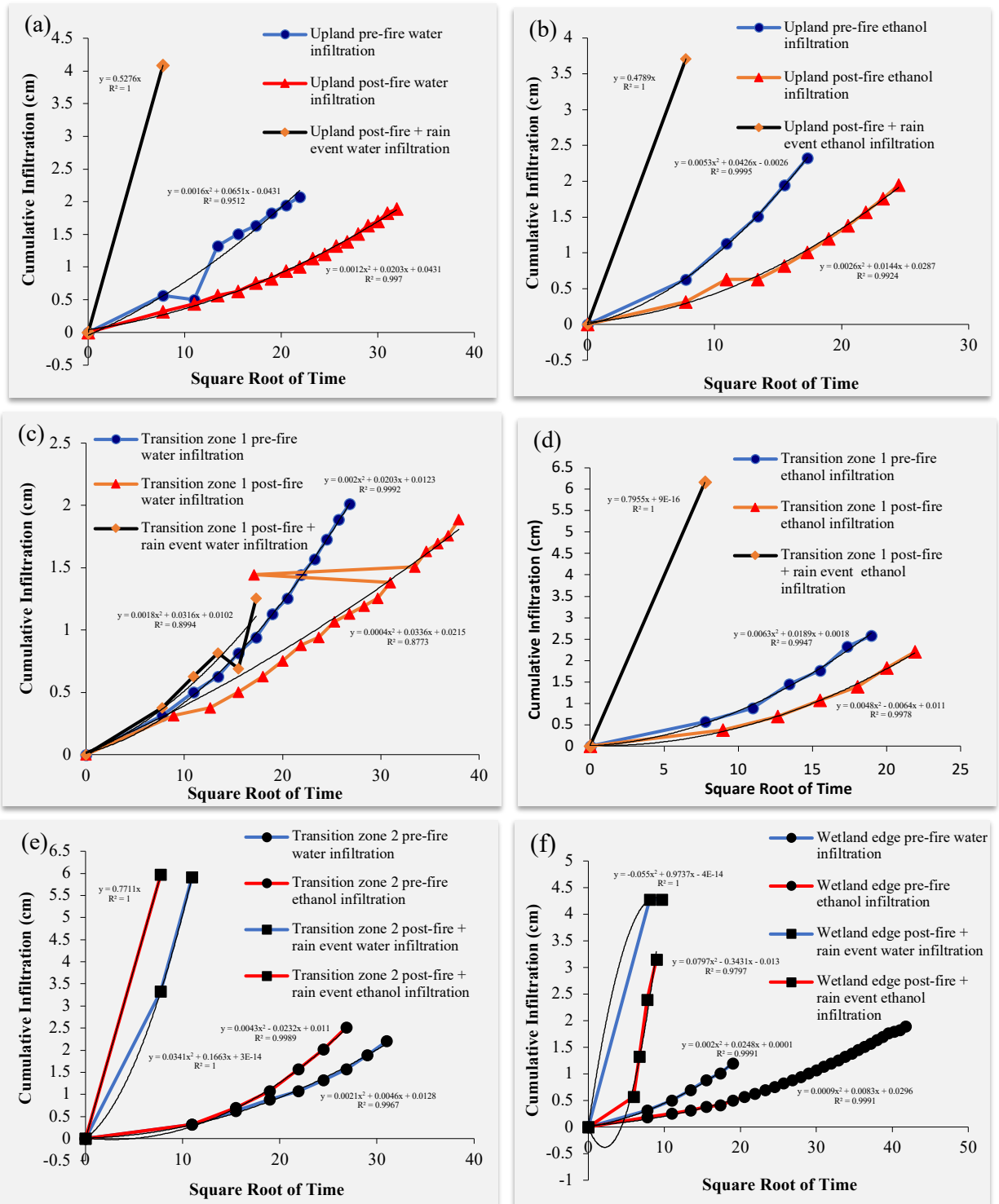


Figure B1. Immediate site upland (a,b) and transition zone 1 (c,d) water and ethanol infiltration rate per square root of time pre-fire (blue line ●), post-fire (red line ▲), and post-fire with rain event included (dark line ◆). Transition zone 2 (e) and wetland edge (f) pre-fire water infiltration rate (blue line ●), pre-fire ethanol infiltration rate (red line ●) including post-fire water infiltration rate (blue line ■) and post-fire ethanol infiltration rate (red line ■).

B.1. Water Infiltration Raw Data

Table B1. Water infiltration data for upland area in immediate site.

UPLAND (PRE-FIRE)	Time (s)	Square Root of time	Volume (ml)	Infiltration (cm)
	0	0	98	0
	60	7.745966692	89	0.565884242
	120	10.95445115	90	0.503008215
	180	13.41640786	77	1.320396565
	240	15.49193338	74	1.509024646
	300	17.32050808	72	1.634776699
	360	18.97366596	69	1.82340478
	420	20.49390153	67	1.949156834
	480	21.9089023	65	2.074908888
UPLAND (POST-FIRE)	Time (s)	Square Root of time	Volume (ml)	Infiltration (cm)
	0	0	81	0
	60	7.745966692	76	0.314380135
	120	10.95445115	74	0.440132188
	180	13.41640786	72	0.565884242
	240	15.49193338	71	0.628760269
	300	17.32050808	69	0.754512323
	360	18.97366596	68	0.81738835
	420	20.49390153	66	0.943140404
	480	21.9089023	65	1.00601643
	540	23.23790008	63	1.131768484
	600	24.49489743	62	1.194644511
	660	25.69046516	60	1.320396565
	720	26.83281573	59	1.383272592
	780	27.92848009	57	1.509024646
	840	28.98275349	55	1.634776699
	900	30	54	1.697652726
	960	30.98386677	52	1.82340478
	1020	31.93743885	51	1.886280807
UPLAND (POST-FIRE + RAIN EVENT)	Time (s)	Square Root of time	Volume (ml)	Infiltration (cm)
	0	0	100	0
	60	7.745966692	35	4.086941749

Table B2. Water infiltration data for transition zone 1 in immediate site.

TRANSITION ZONE 1 (PRE-FIRE)	Time (s)	Square Root of time	Volume (ml)	Infiltration (cm)
	0	0	60	0
	60	7.745966692	55	0.314380135
	120	10.95445115	52	0.503008215
	180	13.41640786	50	0.628760269
	240	15.49193338	47	0.81738835
	300	17.32050808	45	0.943140404
	360	18.97366596	42	1.131768484
	420	20.49390153	40	1.257520538
	480	21.9089023	37	1.446148619
	540	23.23790008	35	1.571900673
	600	24.49489743	32.5	1.72909074
	660	25.69046516	30	1.886280807
	720	26.83281573	28	2.012032861
TRANSITION ZONE 1 (POST-FIRE)	Time (s)	Square Root of time	Volume (ml)	Infiltration (cm)
	0	0	82	0
	80	8.94427191	77	0.314380135
	160	12.64911064	76	0.377256161
	240	15.49193338	74	0.503008215
	325	18.02775638	72	0.628760269
	400	20	70	0.754512323
	480	21.9089023	68	0.880264377
	560	23.66431913	67	0.943140404
	640	25.29822128	65	1.068892457
	720	26.83281573	64	1.131768484
	800	28.28427125	63	1.194644511
	880	29.66479395	62	1.257520538
	960	30.98386677	60	1.383272592
	292	17.08800749	59	1.446148619
	1120	33.46640106	58	1.509024646
	1200	34.64101615	56	1.634776699
	1280	35.77708764	55	1.697652726
	1360	36.87817783	54	1.760528753
	1440	37.94733192	52	1.886280807
TRANSITION ZONE 1 (POST-FIRE + RAIN EVENT)	Time (s)	Square Root of time	Volume (ml)	Infiltration (cm)
	0	0	78	0
	60	7.745966692	72	0.377256161
	120	10.95445115	68	0.628760269
	180	13.41640786	65	0.81738835
	240	15.49193338	67	0.691636296
	300	17.32050808	58	1.257520538

Table B3. Water infiltration data for transition zone 2 in immediate site.

TRANSITION ZONE 2 (PRE-FIRE)	Time (s)	Square Root of time	Volume (ml)	Infiltration (cm)
	0	0	81	0
	120	10.95445115	76	0.314380135
	240	15.49193338	71	0.628760269
	360	18.97366596	67	0.880264377
	480	21.9089023	64	1.068892457
	600	24.49489743	60	1.320396565
	720	26.83281573	56	1.571900673
	840	28.98275349	51	1.886280807
	960	30.98386677	46	2.200660942
TRANSITION ZONE 2 (POST-FIRE + RAIN EVENT)	Time (s)	Square Root of time	Volume (ml)	Infiltration (cm)
	0	0	100	0
	60	7.745966692	47	3.332429426
	120	10.95445115	6	5.910346529

Table B4. Water infiltration data for wetland edge in immediate site.

WETLAND EDGE (PRE-FIRE)	Time (s)	Square Root of time	Volume (ml)	Infiltration (cm)
	0	0	86	0
	60	7.745966692	81	0.314380135
	120	10.95445115	78	0.503008215
	180	13.41640786	75	0.691636296
	240	15.49193338	72	0.880264377
	300	17.32050808	70	1.00601643
	360	18.97366596	67	1.194644511
WETLAND EDGE (POST-FIRE + RAIN EVENT)	Time (s)	Square Root of time	Volume (ml)	Infiltration (cm)
	0	0	100	0
	65	8.062257748	32	4.275569829
	93	9.643650761	32	4.275569829

B.2. Ethanol Infiltration Raw Data

Table B5. Ethanol infiltration for upland area in immediate site.

UPLAND (PRE-FIRE)	Time (s)	Square Root of time	Volume (ml)	Infiltration (cm)
	0	0	62	0
	60	7.745966692	52	0.628760269
	120	10.95445115	44	1.131768484
	180	13.41640786	38	1.509024646
	240	15.49193338	31	1.949156834
	300	17.32050808	25	2.326412995
UPLAND (POST-FIRE)	Time (s)	Square Root of time	Volume (ml)	Infiltration (cm)
	0	0	50	0
	60	7.745966692	45	0.314380135
	120	10.95445115	40	0.628760269
	180	13.41640786	40	0.628760269
	240	15.49193338	37	0.81738835
	300	17.32050808	34	1.00601643
	360	18.97366596	31	1.194644511
	420	20.49390153	28	1.383272592
	480	21.9089023	25	1.571900673
	540	23.23790008	22	1.760528753
	600	24.49489743	19	1.949156834
UPLAND (POST-FIRE + RAIN EVENT)	Time (s)	Square Root of time	Volume (ml)	Infiltration (cm)
	0	0	100	0
	60	7.745966692	41	3.709685587

Table B6. Ethanol infiltration data for transition zone 1 in immediate site.

TRANSITION ZONE 1 (PRE-FIRE)	Time (s)	Square Root of time	Volume (ml)	Infiltration (cm)
	0	0	70	0
	60	7.745966692	61	0.565884242
	120	10.95445115	56	0.880264377
	180	13.41640786	47	1.446148619
	240	15.49193338	42	1.760528753
	300	17.32050808	33	2.326412995
	360	18.97366596	29	2.577917103
TRANSITION ZONE 1 (POST-FIRE)	Time (s)	Square Root of time	Volume (ml)	Infiltration (cm)
	0	0	78	0
	80	8.94427191	72	0.377256161
	160	12.64911064	67	0.691636296
	240	15.49193338	61	1.068892457
	325	18.02775638	56	1.383272592
	400	20	49	1.82340478
	480	21.9089023	43	2.200660942
TRANSITION ZONE 1 (POST-FIRE + RAIN EVENT)	Time (s)	Square Root of time	Volume (ml)	Infiltration (cm)
	0	0	100	0
	60	7.745966692	2	6.161850636

Table B7. Ethanol infiltration data for transition zone 2 in immediate site.

TRANSITION ZONE 2 (PRE-FIRE)	Time (s)	Square Root of time	Volume (ml)	Infiltration (cm)
	0	0	76	0
	120	10.95445115	71	0.314380135
	240	15.49193338	65	0.691636296
	360	18.97366596	59	1.068892457
	480	21.9089023	51	1.571900673
	600	24.49489743	44	2.012032861
	720	26.83281573	36	2.515041076
TRANSITION ZONE 2 (POST-FIRE + RAIN EVENT)	Time (s)	Square Root of time	Volume (ml)	Infiltration (cm)
	0	0	100	0
	60	7.745966692	5	5.973222556

Table B8. Ethanol infiltration data for wetland edge in immediate site.

WETLAND EDGE (PRE-FIRE)	Time (s)	Square Root of time	Volume (ml)	Infiltration (cm)
	0	0	86	0
	60	7.745966692	83	0.188628081
	120	10.95445115	82	0.251504108
	180	13.41640786	81	0.314380135
	240	15.49193338	80	0.377256161
	300	17.32050808	79.5	0.408694175
	360	18.97366596	78	0.503008215
	420	20.49390153	77	0.565884242
	480	21.9089023	76	0.628760269
	540	23.23790008	75	0.691636296
	600	24.49489743	74	0.754512323
	660	25.69046516	73	0.81738835
	720	26.83281573	72	0.880264377
	780	27.92848009	71	0.943140404
	840	28.98275349	70	1.00601643
	900	30	69	1.068892457
	960	30.98386677	68	1.131768484
	1020	31.93743885	67	1.194644511
	1080	32.86335345	66	1.257520538
	1140	33.76388603	65	1.320396565
	1200	34.64101615	64	1.383272592
	1260	35.4964787	63	1.446148619
	1320	36.33180425	62	1.509024646
	1380	37.14835124	61	1.571900673
	1440	37.94733192	60	1.634776699
	1500	38.72983346	59	1.697652726
	1560	39.49683532	58	1.760528753
	1620	40.24922359	57.5	1.791966767
	1680	40.98780306	57	1.82340478
	1740	41.71330723	56	1.886280807
WETLAND EDGE (POST-FIRE + RAIN EVENT)	Time (s)	Square Root of time	Volume (ml)	Infiltration (cm)
	25	0	50	0
	35	5.916079783	41	0.565884242
	45	6.708203932	29	1.320396565
	60	7.745966692	12	2.389289022
	80	8.94427191	0	3.143801345

B.3. Statistical Analysis

Table B9. Unpaired t-test results for the difference in unsaturated hydraulic conductivity in upland and transition Zone 1 comparison in immediate site pre-fire and immediately post-fire (before minus after).

Variables		
Pre-fire X Immediately Post-fire		
	Pre-fire	Immediately Post-fire
Mean	-3.104436153	-3.620014129
Variance	0.000607048	0.135136231
df	2	
t Stat	1.97902002	
P(T<=t) one-tail	0.09319431	
t Critical one-tail	2.91998558	
P(T<=t) two-tail	0.18638863	
t Critical two-tail	4.30265273	
Pre-fire X Post-fire + Rain Event		
	Pre-fire	Post-fire +Rain Event
Mean	-3.104436153	-2.344116765
Variance	0.000607048	1.254553476
df	2	
t Stat	-0.959757306	
P(T<=t) one-tail	0.219226779	
t Critical one-tail	2.91998558	
P(T<=t) two-tail	0.438453557	
t Critical two-tail	4.30265273	

Table B10. Unpaired t-test results for the difference in water repellency, also referred to as hydrophobicity, in immediate site before and immediately after the fire (before minus after).

	Variables	
	Pre-fire	Immediately Post-fire
Pre-fire X Immediately Post-fire		
Mean	0.773691571	1.061503881
Variance	0.000429456	0.374373279
df	2	
t Stat	-0.647536874	
P(T<=t) one-tail	0.291843831	
t Critical one-tail	2.91998558	
P(T<=t) two-tail	0.583687662	
t Critical two-tail	4.30265273	
Pre-fire X Post-fire + Rain Event		
	Pre-fire	Post-fire + Rain Event
Mean	0.773691571	1.662398358
Variance	0.000429456	3.766764507
df	2	
t Stat	-0.66484895	
P(T<=t) one-tail	0.287275253	
t Critical one-tail	2.91998558	
P(T<=t) two-tail	0.574550505	
t Critical two-tail	4.30265273	

APPENDIX C: NUTRIENTS

C.1. Statistical Analysis

Table C1. Unpaired t-test results for the difference in nutrients in soil A horizon before and after the rain event (before minus after).

	Immediate	Chronic
C		
Mean	0.16	-0.29
Variance	0.030466667	0.074066667
df	6	
t Stat	2.783653084	
P(T<=t) one-tail	0.015921539	
t Critical one-tail	1.943180281	
P(T<=t) two-tail	0.031843078	
t Critical two-tail	2.446911851	
P		
Mean	-0.008485	-0.00268
Variance	0.000261512	0.000186354
df	6	
t Stat	-0.548602728	
P(T<=t) one-tail	0.301538616	
t Critical one-tail	1.943180281	
P(T<=t) two-tail	0.603077233	
t Critical two-tail	2.446911851	
K		
Mean	-0.0088825	0.00103
Variance	0.000136312	0.000123329
df	6	
t Stat	-1.230344741	
P(T<=t) one-tail	0.132306493	
t Critical one-tail	1.943180281	
P(T<=t) two-tail	0.264612986	
t Critical two-tail	2.446911851	2.446911851
Mn		
Mean	-0.2303325	0.005905
Variance	0.002830633	0.001493084
df	6	
t Stat	-7.185387496	
P(T<=t) one-tail	0.000183681	
t Critical one-tail	1.943180281	
P(T<=t) two-tail	0.000367362	
t Critical two-tail	2.446911851	
Fe		
Mean	0.341405	0.65976
Variance	0.666862651	0.760141012
df	6	
t Stat	-0.533002354	
P(T<=t) one-tail	0.306593181	
t Critical one-tail	1.943180281	
P(T<=t) two-tail	0.613186363	
t Critical two-tail	2.446911851	
Ca		
Mean	-0.221195	-0.065065
Variance	0.101423873	0.061560938
df	6	

t Stat	-0.77346878	
P(T<=t) one-tail	0.2343066	
t Critical one-tail	1.943180281	
P(T<=t) two-tail	0.468613201	
t Critical two-tail	2.446911851	
<hr/>		
Mg		
Mean	-0.049715	-0.0131625
Variance	0.005569512	0.003675271
df	6	
t Stat	-0.760324062	
P(T<=t) one-tail	0.237933271	
t Critical one-tail	1.943180281	
P(T<=t) two-tail	0.475866541	
t Critical two-tail	2.446911851	
<hr/>		
Na		
Mean	-0.0036475	-0.0021525
Variance	0.000341517	4.51258E-05
df	6	
t Stat	-0.152060502	
P(T<=t) one-tail	0.44206177	
t Critical one-tail	1.943180281	
P(T<=t) two-tail	0.884123539	
t Critical two-tail	2.446911851	
<hr/>		
Al		
Mean	-0.2712925	0.656245
Variance	0.205093759	0.441887536
df	6	
t Stat	-2.306298996	
P(T<=t) one-tail	0.030287619	
t Critical one-tail	1.943180281	
P(T<=t) two-tail	0.060575238	
t Critical two-tail	2.446911851	
<hr/>		
Organic C		
Mean	-0.013760346	0.041222027
Variance	0.240367437	0.055775683
df	6	
t Stat	-0.202070375	
P(T<=t) one-tail	0.423269497	
t Critical one-tail	1.943180281	
P(T<=t) two-tail	0.846538994	
t Critical two-tail	2.446911851	
<hr/>		

Table C2. Unpaired t-test results for the difference in nutrients in soil B horizon before and after the rain event (before minus after).

	Immediate	Chronic
C		
Mean	0.0575	0.04
Variance	0.008891667	0.0202
df	6	
t Stat	0.205203018	
P(T<=t) one-tail	0.42209909	
t Critical one-tail	1.943180281	
P(T<=t) two-tail	0.84419818	
t Critical two-tail	2.446911851	
P		
Mean	0.00364	-0.0082825
Variance	9.56074E-05	0.000388484
df	6	
t Stat	1.083761656	
P(T<=t) one-tail	0.160043808	
t Critical one-tail	1.943180281	
P(T<=t) two-tail	0.320087617	
t Critical two-tail	2.446911851	
K		
Mean	-0.00138	-0.008015
Variance	0.000174058	0.000469231
df	6	
t Stat	0.5232003	
P(T<=t) one-tail	0.309793186	
t Critical one-tail	1.943180281	
P(T<=t) two-tail	0.619586373	
t Critical two-tail	2.446911851	
Mn		
Mean	-0.0178475	0.0425925
Variance	0.000403894	0.003134002
df	6	
t Stat	-2.032272257	
P(T<=t) one-tail	0.044192603	
t Critical one-tail	1.943180281	
P(T<=t) two-tail	0.088385207	
t Critical two-tail	2.446911851	
Fe		
Mean	-0.6670225	0
Variance	1.984558138	0
df	6	
t Stat	-0.946975115	
P(T<=t) one-tail	0.19010608	
t Critical one-tail	1.943180281	
P(T<=t) two-tail	0.380212159	
t Critical two-tail	2.446911851	
Ca		
Mean	-0.075305	-0.026945
Variance	0.007368092	0.00843875
df	6	
t Stat	-0.769296454	
P(T<=t) one-tail	0.23545355	

t Critical one-tail	1.943180281	
P(T<=t) two-tail	0.470907099	
t Critical two-tail	2.446911851	
Mg		
Mean	-0.02921	-0.03438
Variance	0.00162882	0.003215763
df	6	
t Stat	0.148556735	
P(T<=t) one-tail	0.443385251	
t Critical one-tail	1.943180281	
P(T<=t) two-tail	0.886770502	
t Critical two-tail	2.446911851	
Na		
Mean	-0.0125675	-0.00701
Variance	0.000383551	0.000116755
df	6	
t Stat	-0.496925863	
P(T<=t) one-tail	0.318460802	
t Critical one-tail	1.943180281	
P(T<=t) two-tail	0.636921603	
t Critical two-tail	2.446911851	
Al		
Mean	0.0150475	0
Variance	2.760651497	0
df	6	
t Stat	0.018112924	
P(T<=t) one-tail	0.493068033	
t Critical one-tail	1.943180281	
P(T<=t) two-tail	0.986136065	
t Critical two-tail	2.446911851	
Organic C		
Mean	0.18157052	-0.028593534
Variance	0.129882404	0.114811155
df	6	
t Stat	0.849722586	
P(T<=t) one-tail	0.214038448	
t Critical one-tail	1.943180281	
P(T<=t) two-tail	0.428076896	
t Critical two-tail	2.446911851	

Table C3. Two-way ANOVA analysis for nutrient pools in soil A horizon within samples (sampling times) and between sites (columns).

	SS	df	MS	F	P-value	F crit
C						
Sample (Sampling times)	0.0169	1	0.0169	0.079867675	0.782292351	4.747225347
Columns (Sites)	0.0196	1	0.0196	0.092627599	0.766076206	4.747225347
P						
Sample (Sampling times)	0.000124657	1	0.000124657	0.751034722	0.40314465	4.747225347
Columns (Sites)	0.0028896	1	0.0028896	17.40925927	0.001293804	4.747225347
K						
Sample (Sampling times)	6.16618E-05	1	6.16618E-05	0.620399921	0.446178328	4.747225347
Columns (Sites)	0.000991778	1	0.000991778	9.978611623	0.008237749	4.747225347
Mn						
Sample (Sampling times)	0.003286442	1	0.003286442	0.579814881	0.461087946	4.747225347
Columns (Sites)	0.145960292	1	0.145960292	25.75123582	0.000273109	4.747225347
Fe						
Sample (Sampling times)	1.002331357	1	1.002331357	1.579590921	0.232733242	1.002331357
Columns (Sites)	7.30891225	1	7.30891225	11.5182383	0.005329913	7.30891225
Ca						
Sample (Sampling times)	0.081944788	1	0.081944788	2.028343517	0.179870483	4.747225347
Columns (Sites)	0.015640004	1	0.015640004	0.387130174	0.54545282	4.747225347
Mg						
Sample (Sampling times)	0.00395358	1	0.00395358	1.655624154	0.222463709	4.747225347
Columns (Sites)	0.015864032	1	0.015864032	6.643314397	0.024210615	4.747225347
Na						
Sample (Sampling times)	3.364E-05	1	3.364E-05	0.273932083	0.610235456	4.747225347
Columns (Sites)	0.000273572	1	0.000273572	2.227706247	0.161372372	4.747225347
Al						
Sample (Sampling times)	0.148188427	1	0.148188427	0.26931912	0.613225562	4.747225347
Columns (Sites)	26.62170434	1	26.62170434	48.38255002	1.52623E-05	4.747225347
Organic C						
Sample (Sampling times)	0.000754144	1	0.000754144	0.007774347	0.931194136	4.747225347
Columns (Sites)	5.05143E-05	1	5.05143E-05	0.000520744	0.982169069	4.747225347

Table C4. Two-way ANOVA analysis for nutrient pools in soil B horizon within samples (sampling times) and between sites (columns).

	SS	df	MS	F	P-value	F crit
C						
Sample (Sampling times)	0.00950625	1	0.00950625	0.530149878	0.480511163	4.747225347
Columns (Sites)	0.00455625	1	0.00455625	0.254095504	0.623332865	4.747225347
P						
Sample (Sampling times)	2.15528E-05	1	2.15528E-05	0.080488603	0.781471833	4.747225347
Columns (Sites)	0.00573314	1	0.00573314	21.41031692	0.000582978	4.747225347
K						
Sample (Sampling times)	8.8266E-05	1	8.8266E-05	0.453297917	0.513531274	4.747225347
Columns (Sites)	0.005614505	1	0.005614505	28.83378262	0.000168138	4.747225347
Mn						
Sample (Sampling times)	0.000612315	1	0.000612315	0.321010028	0.5814437	4.747225347
Columns (Sites)	0.006372829	1	0.006372829	3.340995892	0.092529095	4.747225347
Fe						
Sample (Sampling times)	0.444919016	1	0.444919016	0.141207511	0.713642221	4.747225347
Columns (Sites)	17.4144089	1	17.4144089	5.526950424	0.036649557	4.747225347
Ca						
Sample (Sampling times)	0.010455063	1	0.010455063	1.83155874	0.200888104	4.747225347
Columns (Sites)	0.001871428	1	0.001871428	0.327844006	0.577501944	4.747225347
Mg						
Sample (Sampling times)	0.004043688	1	0.004043688	2.626835227	0.131034389	4.747225347
Columns (Sites)	0.028586356	1	0.028586356	18.57008852	0.001015088	4.747225347
Na						
Sample (Sampling times)	0.000383279	1	0.000383279	2.238173391	0.160469707	4.747225347
Columns (Sites)	0.000489626	1	0.000489626	2.859196225	0.116637708	4.747225347
Al						
Sample (Sampling times)	0.000226427	1	0.000226427	2.26595E-05	0.996280146	4.747225347
Columns (Sites)	152.5707923	1	152.5707923	15.26836949	0.00208173	4.747225347
Organic C						
Sample (Sampling times)	0.023401958	1	0.023401958	0.145338625	0.709694325	4.747225347
Columns (Sites)	0.611606828	1	0.611606828	3.798404151	0.075065044	4.747225347

Table C5. Eigenvectors values from principal component analysis.

	Prin1	Prin2	Prin3	Prin4	Prin5	Prin6	Prin7	Prin8	Prin9	Prin10
Total C (%)	0.35033	-0.35589	0.21163	0.30818	-0.11476	-0.21666	0.31076	-0.19986	0.27167	0.58345
Total P (mg/g)	0.44599	0.08860	-0.07660	0.24628	0.03897	0.08524	0.54979	0.29817	-0.52669	-0.22219
Total K (mg/g)	0.21146	0.57650	-0.04766	0.02564	-0.15625	0.05266	0.27010	0.00772	0.67969	-0.24046
Total Mn (mg/g)	0.36452	-0.12916	0.41184	-0.08966	0.20107	0.14756	-0.09873	-0.63170	-0.04839	-0.44660
Total Fe (mg/g)	-0.17982	-0.31708	0.52812	-0.25211	0.14982	0.39026	0.26580	0.46537	0.24198	-0.06428
Total Ca (mg/g)	0.40823	-0.05033	0.16903	-0.32379	0.04602	-0.65802	-0.27723	0.40250	0.05660	-0.14222
Total Mg (mg/g)	0.26176	0.46245	0.16503	-0.49578	0.05459	0.26812	-0.05574	-0.05273	-0.23188	0.55683
Total Na (mg/g)	-0.15698	0.21826	0.55935	0.24795	-0.68712	-0.05462	-0.14881	0.04726	-0.22359	-0.06234
Total Al (mg/g)	-0.19190	0.37726	0.34494	0.46914	0.64847	-0.18808	-0.09218	0.07039	-0.01524	0.11045
Organic C (%)	0.41448	-0.09778	-0.10436	0.37403	-0.01687	0.47508	-0.58069	0.28898	0.13683	0.04943

APPENDIX D: CARBON AND NITROGEN ISOTOPIC RATIOS

D.1. Carbon and Nitrogen Isotopic Ratios Raw Data

Table D1. Carbon and nitrogen isotopic ratios in immediate and chronic sites.

IMMEDIATE SITE					
SAMPLING TIME 1	$\delta^{13}\text{C}/^{12}\text{C}$ (‰)	$\delta^{15}\text{N}/^{14}\text{N}$ (‰)	SAMPLING TIME 2	$\delta^{13}\text{C}/^{12}\text{C}$ (‰)	$\delta^{15}\text{N}/^{14}\text{N}$ (‰)
Upland			Upland		
A1	-26.39	1.26	A1	-26.54	4.08
A3	-24.57	7.88	A3	-24.41	9.10
Transition Zone 1			Transition Zone 1		
B1	-25.76	2.61	B1	-25.06	2.65
B4	-24.46	8.39	B4	-23.03	7.92
Transition Zone 2			Transition Zone 2		
C1	-26.80	2.57	C1	-26.00	5.05
C3	-25.63	6.71	C3	-24.91	8.47
Wetland Edge			Wetland Edge		
D1	-26.30	1.99	D1	-26.78	-1.22
D2	-25.11	6.98	D2	-24.73	7.49
CHRONIC SITE					
SAMPLING TIME 1	$\delta^{13}\text{C}/^{12}\text{C}$ (‰)	$\delta^{15}\text{N}/^{14}\text{N}$ (‰)	SAMPLING TIME 2	$\delta^{13}\text{C}/^{12}\text{C}$ (‰)	$\delta^{15}\text{N}/^{14}\text{N}$ (‰)
Upland			Upland		
E1	-25.32	3.85	E1	-26.28	3.42
E3	-24.22	7.30	E3	-23.93	9.70
Transition Zone 1			Transition Zone 1		
F1	-24.07	4.30	F1	-23.98	-3.40
F3	-23.06	8.45	F3	-23.43	7.78
Transition Zone 2			Transition Zone 2		
G1	-25.07	2.57	G1	-25.17	-1.24
G3	-23.88	7.02	G3	-23.24	9.47
Wetland Edge			Wetland Edge		
H1	-24.28	1.47	H1	-24.17	-1.90
H3	-22.72	7.45	H3	-24.04	6.77

D.2. Statistical Analysis

Table D2. Two-way ANOVA analysis for carbon and nitrogen isotopic ratios in soil A horizon within samples (sampling times) and between sites (columns).

	SS	df	MS	F	P-value	F crit
Carbon Isotopic Ratio						
Sample (Sampling times)	9.65257E-07	1	9.65257E-07	1.70688E-06	0.998979051	4.747225347
Columns (Sites)	8.000469527	1	8.000469527	14.1473758	0.002714481	4.747225347
Nitrogen Isotopic Ratio						
Sample (Sampling times)	10.99688498	1	10.99688498	2.414445891	0.146185715	4.747225347
Columns (Sites)	6.026762318	1	6.026762318	1.323219397	0.27242299	4.747225347

Table D3. Two-way ANOVA analysis for carbon and nitrogen isotopic ratios in soil B horizon within samples (sampling times) and between sites (columns).

	SS	df	MS	F	P-value	F crit
Carbon Isotopic Ratio						
Sample (Sampling times)	0.229337069	1	0.229337069	0.554984248	0.470627727	4.747225347
Columns (Sites)	4.349335276	1	4.349335276	10.52517406	0.007030969	4.747225347
Nitrogen Isotopic Ratio						
Sample (Sampling times)	2.658113021	1	2.658113021	3.083629518	0.104549628	4.747225347
Columns (Sites)	0.060700197	1	0.060700197	0.070417216	0.795233963	4.747225347

Table D4. Unpaired t-test results for the difference in carbon and nitrogen isotopic ratios in soil A horizon before and after the rain event (before minus after).

	Immediate	Chronic
Carbon Isotopic Ratio		
Mean	-0.2113572	0.212339675
Variance	0.412079724	0.253779987
df	6	
t Stat	-1.038469839	
P(T<=t) one-tail	0.169539069	
t Critical one-tail	1.943180281	
P(T<=t) two-tail	0.339078139	
t Critical two-tail	2.446911851	
Nitrogen Isotopic Ratio		
Mean	-0.513869775	3.830024925
Variance	7.641886024	8.910503364
df	6	
t Stat	-2.13539852	
P(T<=t) one-tail	0.038317901	
t Critical one-tail	1.943180281	
P(T<=t) two-tail	0.076635802	
t Critical two-tail	2.446911851	

Table D5. Unpaired t-test results for the difference in carbon and nitrogen isotopic ratios in soil B horizon before and after the rain event (before minus after).

	Immediate	Chronic
Carbon Isotopic Ratio		
Mean	-0.6710835	0.192192
Variance	0.306935344	0.741707145
df	6	
t Stat	-1.686031507	
P(T<=t) one-tail	0.071382781	
t Critical one-tail	1.943180281	
P(T<=t) two-tail	0.142765561	
t Critical two-tail	2.446911851	
Nitrogen Isotopic Ratio		
Mean	-0.755456625	-0.874915425
Variance	0.93589427	3.19554367
df	6	
t Stat	0.117543205	
P(T<=t) one-tail	0.455132849	
t Critical one-tail	1.943180281	
P(T<=t) two-tail	0.910265698	
t Critical two-tail	2.446911851	